Received: 10 June 2020 | Revised: 30 August 2021 | Accepted: 1 September 2021 | Published on: 12 October 2021

DOI: 10.1002/joc.7378

International Journal of Climatology RMetS

RESEARCH ARTICLE

Observed and projected trends in climate extremes in a tropical highland region: An agroecosystem perspective

Dereje Ademe Birhan[1,2,3] | **Benjamin F. Zaitchik**[2] | **Kindie Tesfaye Fantaye**[4] | **Belay Simane Birhanu**[5] | **Getachew Alemayehu Damot**[3] | **Enyew Adgo Tsegaye**[3]

[1]College of Agriculture and Natural Resources, Debre Markos University, Debre Markos, Ethiopia

[2]Department of Earth and Planetary Sciences, Johns Hopkins University, Baltimore, Maryland, USA

[3]College of Agriculture and Environmental Science, Bahir Dar University, Bahir Dar, Ethiopia

[4]Integrated Development Program (IDP), International Maize and Wheat Improvement Center (CMMYT), Addis Ababa, Ethiopia

[5]College of Development Studies (Center for Environment and Development Studies), Addis Ababa University, Addis Ababa, Ethiopia

Correspondence
Dereje Ademe, College of Agriculture and Natural Resources, Debre Markos University, Debre Markos, Ethiopia.
Email: ademe.dereje@gmail.com

Funding information
National Science Foundation (NSF), Grant/Award Number: 1624335

Abstract

Tropical highland environments present substantial challenges for climate projections due to sparse observations, significant local heterogeneity and inconsistent performance of global climate models (GCMs). Moreover, these areas are often densely populated, with agriculture-based livelihoods sensitive to transient climate extremes not always included in available climate projections. In this context, we present an analysis of observed and projected trends in temperature and precipitation extremes across agroecosystems (AESs) in the northwest Ethiopian Highlands, to provide more relevant information for adaptation. Limited observational networks are supplemented with a satellite-station hybrid product, and trends are calculated locally and summarized at the adaptation-relevant unit of the AES. Projections are then presented from GCM realizations with divergent climate projections, and results are interpreted in the context of agricultural climate sensitivities. Trends in temperature extremes (1981–2016) are typically consistent across sites and AES, but with different implications for agricultural activities in the other AES. Trends in temperature extremes from GCM projected data also generally have the same sign as the observed trends. For precipitation extremes, there is greater site-to-site variability. Summarized by AES, however, there is a clear tendency towards reduced precipitation, associated with decreases in wet extremes and a tendency towards temporally clustered wet and dry days. Over the retrospective analysis period, neither of the two analysed GCMs captures these trends. Future projections from both GCMs include significant wetting and an increase in precipitation extremes across AES. However, given the lack of agreement between GCMs and observations with respect to trends in recent decades, the reliability of these projections is questionable. The present study is consistent with the "East Africa Paradox" that observations show drying in summer season rainfall while GCMs project wetting. This has an expression in summertime Ethiopian rain that has not received significant attention in previous studies.

KEYWORDS

agriculture, agroecosystem, climate, climate change, climate extremes, Ethiopia

 © 2021 Royal Meteorological Society

10970088, 2022, 4, Downloaded from https://rmets.onlinelibrary.wiley.com/doi/10.1002/joc.7378 by Johns Hopkins University, Wiley Online Library on [28/12/2022]. See the Terms and Conditions (https://onlinelibrary.wiley.com/terms-and-conditions) on Wiley Online Library for rules of use; OA articles are governed by the applicable Creative Commons License

1 | INTRODUCTION

The Ethiopian highlands are topographically and climatically diverse. Mixed subsistence agriculture with limited external input use is the dominant means of livelihood, where both crops and livestock production are integrated in traditional farming systems. Moreover, these areas are highly affected and challenged by climate extremes. Ethiopia, where the study area is located, has a long history of extreme weather events that lead to crop failure, food shortages and reduced or negative economic growth rates (Block *et al*., 2008; World Bank, 2011; Mekasha *et al*., 2014). Although the area receives high rainfall, the rain in these regions is highly variable, and the events tend to be highly erratic and typically come in the form of intense, erosive convective storms (Nyssen *et al*., 2005; Zaitchik *et al*., 2012).

Over the past three decades, Ethiopia has experienced numerous localized drought events and seven major droughts, five of which resulted in famines (Philip et al., 2018). For instance, the 2015/16 drought affected the southeastern and eastern part of our study region and caused significant and widespread acute food insecurity (Philip et al., 2018). There is evidence that climate extreme events, particularly droughts and floods, are on the rise (Mann and Warner, 2017), and the warming climate may cause further increase (Teshome and Zhang, 2019). The anticipated future climate variability and change in extremes could accelerate already high levels of land degradation, soil erosion, deforestation (Fetene *et al*., 2014; Gessesse and Melesse, 2018), loss of biodiversity and recurrent floods, which affect people and infrastructure (World Bank, 2011; Wold Bank, 2019).

Given the exposure of highland agriculture to climatic extremes, there is considerable interest in improving understanding of current and projected trends in climate extremes in this region. At the same time, the highly localized nature of tropical highland climate variability would result in high variability in trends and the agricultural implications of these trends over short distances. This poses a challenge for adaptation-relevant climate projections. It is important not only to characterize trends at a scale that is specific enough to highland agricultural systems but also at a scale that is generally enough to allow for a regional risk assessment and adaptation planning. Moreover, patterns and trends in climate extremes should be interpreted in the context of local agricultural systems to understand how changes in different climate extreme indices (CEI) impact crops and production systems in a given agroecosystem (AES).

The relevance of climate extremes for agriculture, and of CEI used for their characterization, is generally recognized (Vogel *et al*., 2019). Many studies have applied one or a combination of pre-defined CEI to examine trends in extreme events in different regions of the world, including Africa and Ethiopia. Global level studies revealed that temperature-based indices showed a significant increase, and maximum five-day precipitation and 95th percentile of precipitation are projected to increase significantly in most parts of the world (Sillmann and Roeckner, 2008). De los Milagros Skansi *et al*. (2013) reported a significant warming and wetting across the whole of South America since the mid-20th century onwards. A study conducted in Georgia also showed an overall increase in precipitation and temperature extreme indices (Keggenhoff *et al*., 2014). Mouhamed *et al*. (2013) did a climate extreme study in West African Sahel and reported a general tendency of decreased annual total rainfall and maximum number of consecutive wet days. Gebrechorkos *et al*. (2019) did a climate extreme analysis over East Aftrica using the grided data and reported an overall increasing trend in temperature indices and a mix of decreasing and increasing trends in precipitation indices. Studies conducted on CEI trends in Ethiopia have reported diverse results. Most studies indicate significant increasing trends for temperature indices in recent decades (Mekasha *et al*., 2014; Kiros *et al*., 2017; Esayas *et al*., 2018a). For precipitation, some studies show a decrease in CEI (Gebrechorkos *et al*., 2019), while some studies show a mix of increasing and decreasing trends (Degefu and Bewket, 2014), and some other studies showed increasing trends (Shang *et al*., 2011). These differences could be associated with the differences in spatial and temporal coverage of the studies, particularly considering the local character of climate in the highlands. Thus, localized studies on climate extremes will benefit local farmers whose livelihood is entirely dependent on agricultural activities that necessitate the present study. Appropriate scale and resolution of data are also critical. Several studies, to date, in the region have concentrated on the analysis of indices for climate extremes based on observational data from a very limited set of weather stations. While others covered very large areas, averaging over local heterogeneities, others focused primarily on the changes of extremes in future climate projections (Sillmann and Roeckner, 2008). The limitations of climate extreme studies in the area are well documented in Gebrechorkos *et al*. (2019).

Unlike many other studies, our analysis considers the unique differences between AES, and results are interpreted in terms of their implications for agricultural activities in each AES. We also focus on climate extreme indices deemed most relevant for local agriculture, and adjust CEI thresholds where necessary to match relevant indicators for local crops. Applying this perspective, our analysis aimed to (i) analyse recent (1981–2016) observed trends in precipitation and temperature extremes over a tropical highland region based on AES, (ii) assess the performance of selected global climate models (GCMs) to

10970088, 2022, 4, Downloaded from https://rmets.onlinelibrary.wiley.com/doi/10.1002/joc.7378 by Johns Hopkins University, Wiley Online Library on [28/12/2022]. See the Terms and Conditions (https://onlinelibrary.wiley.com/terms-and-conditions) on Wiley Online Library for rules of use; OA articles are governed by the applicable Creative Commons License

generate precipitation and temperature extremes, and (iii) examine projections of AES-level changes in precipitation and temperature extremes over the 21st century.

2 | MATERIALS AND METHODS

2.1 | Description of the study site

This study focuses in Choke Mountain and its constituent peaks, located in the Blue Nile Highlands of northwest Ethiopia. The watersheds of Choke Mountain cover an elevation range from 800 to 4,200 masl and are located within geographic coordinates of 9.75°–11.5°N and 37.8°–38.33°E (Figure 1). The study area covers 19,915 km^2, in which 3.1 million people reside, with a population density of 161 people per km^2. Ninety percent of the population lives in rural areas (http://www.csa.gov.et/census-report/complete-report/census-2007). The region is characterized by significant interannual climate variability, complex topography and associated local climate contrasts, erosive rains and erodible soils.

The area also experiences intense land pressure due to an increasing population and agriculture-based economy, which is entirely dependent on smallholder low-input–output agriculture. Farming is predominantly a crop-livestock mixed system that is operated by independent farmers on small plots (Simane *et al*., 2012, 2013; Zaitchik *et al*., 2012). Nitisols, Vertisols, Andosols and Acrisols are dominant soil types of the area (Zaitchik *et al*., 2012). Dry valleys, gently rolling, deep soil midland plains and cool, wet alpine zones are found within a short distance from the mountain, and complex topography leads to strong local contrasts in precipitation and temperature (Zaitchik *et al*., 2012). The topographic climate gradient ranging from warm to cool allows for the production of diverse crops of both tropical and temperate origins, which are highly relevant when considering climate variability. Temperate origin crops at higher elevations benefit from or are entirely dependent on seasonally cold temperatures. Here, we apply the AES as an agriculturally relevant unit of aggregation (Conway, 1985). The AES represents the intersection of a common set of climate conditions, soil properties and farming systems and, thus, offers a unit that is relevant for analysing and communicating impacts of climate on agriculture (Simane *et al*., 2013). A brief description of the AES in the mountain watersheds is presented in Table 1.

2.2 | Study approach

2.2.1 | Data type and source

Records of daily precipitation and minimum and maximum temperature were extracted from the Enhancing National Climate Services (ENACTS) dataset. ENACTS is a 4 × 4 km gridded dataset reconstructed from weather stations and meteorological satellite records from 1981 to 2016 (Dinku *et al*., 2014, 2016). ENACTS has been evaluated extensively and has demonstrated strong performance when evaluated at station locations across the country (Dinku *et al*., 2014, 2016; Alemayehu and Bewket, 2017). For this study, the Ethiopian National

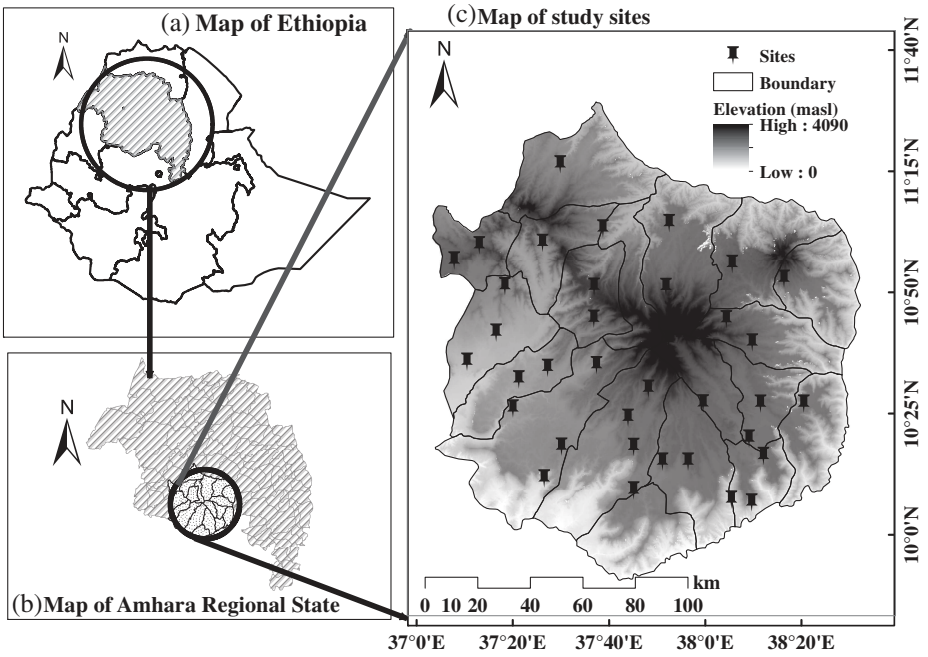

FIGURE 1 Map of the study area

10970088, 2022, 4, Downloaded from https://rmets.onlinelibrary.wiley.com/doi/10.1002/joc.7378 by Johns Hopkins University, Wiley Online Library on [28/12/2022]. See the Terms and Conditions (https://onlinelibrary.wiley.com/terms-and-conditions) on Wiley Online Library for rules of use; OA articles are governed by the applicable Creative Commons License

TABLE 1 Characteristics of agroecosystems of the Choke Mountain watersheds (adapted from Simane *et al*., 2013)

Agroecosystem	Farming system	Traditional climatic zone	Dominant soils	Major crops
AES1: Lowlands and Abay valley	Fragmented sorghum-based extensive	Upper Kola	Leptosols Cambisols	Sorghum, teff, maize, haricot bean
AES2: Midland plains with black soil	Intensive teff-based	Lower Weyna Dega	Vertisols	Teff, durum wheat, barley, chickpea, grass pea
AES3: Midland plains with brown soil	Intensive maize–wheat-based	Lower Weyna Dega	Nitosols Alisols	Wheat, maize, teff
AES4: Midland sloping lands	Semi-intensive wheat/barley based	Upper Weyna Dega—lower Dega	Leptosols Nitosols Alisols	Wheat, teff, barley, Engido (Avena spp.)
AES5: Hilly and mountainous highlands	Potato/barley-based	Upper Dega	Leptosols Luvisols	Potato, barley, faba bean, Engido

Meteorological Agency provided ENACTS data for 36 locations in Choke Mountain. In using a gold standard hybrid gridded product (ENACTS) but doing so for selected locations at which stations are available for direct evaluation of the product, we are able to assemble temporally complete records of confirmed reliability.

All GCM outputs used in this study are drawn from the NEX-GDDP archive, which is a collection of downscaled CMIP5 simulations with a resolution of $0.25^\circ \times 0.25^\circ$. The producers used to prepare the dataset are detailed in (Thrasher *et al*., 2012). Model output used for projecting future trends was obtained from two GCMs that have demonstrated the ability to capture climate teleconnections relevant to the Ethiopian Highlands: MIROC5 and IPSL CM5A LR (Bhattacharjee and Zaitchik, 2015). GCM-derived estimates of daily precipitation and minimum and maximum temperatures were obtained from the NASA Earth Exchange Global Daily Downscaled Projections (*NEX-GDDP*) dataset (van Vuuren *et al*., 2011; Thrasher *et al*., 2012).

We note that these two GCMs do not perform particularly well on conventional metrics of bias with respect to historical observations, but the fact that they are able to capture some elements of large-scale climate influence on the region suggests that they are reasonable choices for generating future projections (Siam and Eltahir, 2017). In addition, the models were selected, because the available realizations of the two models diverge significantly from one to another. In this sense, the two capture the uncertainty present in climate projections for the region. The NEX-GDDP data have been corrected for biases using bias-correction and spatial disaggregation (BCSD), including empirical quantile mapping (Piani *et al*., 2010; Thrasher *et al*., 2012; Maraun, 2016; Cannon, 2018; Navarro-racines *et al*., 2020). The NEX-GDDP bias correction is limited by its reliance on a global reference dataset that is not optimized for Ethiopia. Thus, we perform a second bias correction to adjust NEX-GDDP to ENACT using an additive (delta) method for temperature and multiplication ratio for precipitation data (Berg *et al*., 2012). This makes GCM results statistically consistent with observations and allows us to quantify their projected changes. The bias-corrected GCM data were divided into two parts: near-term projection (2017–2050) and late-21st century projection (2051–2095). For evaluation, we construct a retrospective GCM dataset using the "historical" simulation—i.e., the CMIP5 20th century experiments, which run through 2005—merged with RCP4.5 for 2006–2016 to get records representative of the 1981–2016 period of ENACTS availability.

2.2.2 | Data preparation and quality control

Homogeneity and change points for ENACTS dataset were checked using the penalized maximal F (PMF) test (Wang, 2008a, 2008b). The PMF test is used as the standard homogeneity and change point tests (like standard normal homogeneity [SNH] test) did not detect changes at any location in the data series, and a reference series for the test is not available. RHtestsV3 and RHtests_dlyPrcp software packages were used for temperature and rainfall, respectively. Details of these tools are documented in the literature (Wang *et al*., 2010; Wang and Feng, 2013).

2.2.3 | Climate extreme indices studied

Using the AES as the lens for analysis, we examine a suite of standard CEI in observations and in selected downscaled GCMs, considering both the recent past and projections for the mid- and late-21st century. As

10970088, 2022, 4, Downloaded from https://rmets.onlinelibrary.wiley.com/doi/10.1002/joc.7378 by Johns Hopkins University, Wiley Online Library on [28/12/2022]. See the Terms and Conditions (https://onlinelibrary.wiley.com/terms-and-conditions) on Wiley Online Library for rules of use; OA articles are governed by the applicable Creative Commons License

temperature and precipitation are among the major biophysical factors that affect crop production (Hatfield and Prueger, 2015), we focus on extremes related to these two variables. Accordingly, we calculate a suite of indices defined by the Expert Team on Climate Change Detection and Indices (ETCCDI) (Table 2).

These include two agronomically important indices of temporal rainfall variability, consecutive dry days (CDD) and consecutive wet days (CWD), threshold indices for high ("summertime" = SU) temperature (SU25) and for two levels of daily rainfall extreme (days with more than 10 mm precipitation (R10mm) and 20 mm precipitation (R20mm), nine indices of absolute temperature or rainfall amount (TXx, TNx, TXn, TNn, DTR, Rx1day and Rx5day, prcptot and sdii) and four indices of percentile temperature (TX10p, TX90p, TN10p and TN90p) (Abatan *et al*., 2018). In addition, one regionally specific temperature extreme (threshold index) was defined, which we call "chill days" (FD10). This index was used to examine the number of days when minimum temperature is less than 10°C. This threshold is selected, because it is the base temperature for most tropical crops below which chilling injury may occur, and the upper threshold for the chilling temperature requirement of temperate crops. Many temperate fruits and vegetables require prolonged exposure to a cold (a chilling temperature) to trigger flower bud induction in a process called vernalization (Atkinson *et al*., 2013; Li *et al*., 2013).

2.2.4 | Data analysis

Extremes trend analysis over the retrospective analysis period (1981–2016) was conducted using the Mann-Kendall trend test. Where autocorrelation was not significant, a standard Mann-Kendall trend tests were applied. When serial autocorrelation was found to be significant, a trend test was performed following the modified Mann-Kendall Test. The magnitude of the trend change was estimated using Sens's slope estimator (Mann, 1945; Sen, 1968) as implemented in R-package *Rclimdex 1.0* (Karl *et al*., 1999).

TABLE 2 Definitions of indices used in the study (adapted from Karl *et al*., 1999)

Indices	Type	Name	Definition	Unit
Temperature indices				
SU25	Threshold	Summer days	Annual count of days when TX >25°C	Days
FD10[a]	Threshold	Chill days	Annual count of days when TN <10°C	Days
TXx	Absolute	Max. Tmax/warmest day	Maximum of daily maximum temperature	°C
TXn	Absolute	Max. Tmin/coldest day	Minimum of daily maximum temperature	°C
TNx	Absolute	Min. Tmax/warmest night	Maximum of daily minimum temperature	°C
TNn	Absolute	Min. Tmin/coldest night	Minimum of daily minimum temperature	°C
TX10p	Percentile	Cold days	Percentage of time when daily TX <10th percentile	%
TX90p	Percentile	Warm days	Percentage of time when daily TX >90th percentile	%
TN10p	Percentile	Cold nights	Percentage of time when daily TN <10th percentile	%
TN90p	Percentile	Warm nights	Percentage of time when daily TN >90th percentile	%
DTR	Absolute	Diurnal temperature range	Monthly mean difference between daily max and min	°C
Precipitation indices				
CDD	Duration	Consecutive dry days	Maximum number of consecutive days with RR < 1 mm	Days
CWD	Duration	Consecutive wet days	Maximum number of consecutive days with RR > 1 mm	Days
R10mm	Threshold	Heavy rainfall days	Annual count of days when PRCP ≥ 10 mm	Days
R20mm	Threshold	Very heavy rainfall days	Annual count of days when PRCP ≥ 20 mm	Days
Rx1day	Absolute	Maximum one-day rainfall	Maximum amount of one-day rainfall in a year	Mm
Rx5day	Absolute	Maximum five-day rainfall	Maximum amount of five-day cumulative rainfall in a year	Mm
SDII	Absolute	Simple daily intensity index	Daily precipitation amount on wet days	mm/day
Prcptot	Absolute	Total precipitation	Annual total rainfall in wet days	Mm

Note: TX, TN, and RR are daily maximum temperature, minimum temperature, and rainfall, respectively.
[a]User-defined temperature index.

10970088, 2022, 4, Downloaded from https://rmets.onlinelibrary.wiley.com/doi/10.1002/joc.7378 by Johns Hopkins University, Wiley Online Library on [28/12/2022]. See the Terms and Conditions (https://onlinelibrary.wiley.com/terms-and-conditions) on Wiley Online Library for rules of use; OA articles are governed by the applicable Creative Commons License

The Mann-Kendal test was applied using the formula:

$$S=\sum_{k=1}^{n-1}\sum_{j=k+1}^{n}\operatorname{sgn}\left(x_j-x_k\right) \tag{1}$$

where n = number of data points, x_k and x_j = data values in time series k and j ($j > k$), and $\operatorname{sgn}(x_j - x_k)$ = sign function as:

$$\operatorname{sgn}\left(x_j-x_k\right)=\left\{\begin{array}{ll}1 & \text{if } x_j-x_k>0\\ 0 & \text{if } x_j-x_k=0\\ -1 & \text{if } x_j-x_k<0\end{array}\right\} \tag{2}$$

The variance of S is computed as:

$$\operatorname{VAR}(S)=\frac{\left[n(n-1)(2n+5)-\sum_{p=1}^{q}t_p\left(t_p-1\right)\left(2t_p+5\right)\right]}{18} \tag{3}$$

where q = number of tied groups, and t_p = the number of data points in the pth group.

The values of S and VAR(S) were used to compute the test statistic Z_s as follows:

$$Z_s=\left\{\begin{array}{ll}\dfrac{S-1}{\sqrt{\operatorname{VAR}(S)}} & \text{if } S>0\\ 0 & \text{if } S=0\\ \dfrac{S+1}{\sqrt{\operatorname{VAR}(S)}} & \text{if } S<0\end{array}\right\} \tag{4}$$

Positive/negative Z_s indicates an upward/downward trend for the period.

Sen's slope estimator (Sen, 1968) was used to estimate the slope of the trend. Sen's method can be used in cases where the trend can be assumed to be linear and is equal to:

$$f(t)=Q_t+B \tag{5}$$

where $f(t)$ is a continuous monotonic increasing or decreasing function of time, Q_t is the slope, and B is a constant. The slopes of all data value pairs were calculated to get the slope estimate Q in Equation (3) as:

$$Q_i=\frac{x_j-x_k}{j-k}\ \text{for}\ i=1,\ldots,N \tag{6}$$

where X_j and X_k are the data values at times j and k ($j > k$). Hence, we only have one datum in each period, and N is computed as:

$$N=\frac{n(n-1)}{2} \tag{7}$$

where n is the number of time periods. The N values of Q_i were ranked from smallest to largest, and the median of slope or Sen's estimator was computed as (Gocic and Trajkovic, 2013):

$$Q_{\text{med}}=\left\{\begin{array}{l}Q_{\left[\frac{N+1}{2}\right]}\ \text{if } N \text{ is odd}\\ \dfrac{Q_{\left[\frac{N}{2}\right]}+Q_{\left[\frac{N+2}{2}\right]}}{2}\ \text{if } N \text{ is even}\end{array}\right. . \tag{8}$$

Positive/negative values of Q_i indicate an increasing/decreasing trend, respectively (Salmi et al., 2002). Confidence intervals (C_α) about the time slopes were used to test significance of the trend and were computed as follows (Gilbert, 1987):

$$C_\alpha=z_{1-\alpha/2}\sqrt{\operatorname{Var}(S)} \tag{9}$$

where Var(S) is defined in Equation (3), and $z_{1-\alpha/2}$ is obtained from the standard normal distribution table.

The Wilmot index was used to evaluate the performance of GCMs to reproduce extreme indices compared with indices generated from ENACT data. The Wilmot index of agreement (d) was calculated as (Willmott, 1982):

$$d=1-\left[\frac{\sum_{i=1}^{n}\left(P_i-O_i\right)^2}{\sum_{i=1}^{n}\left(\left|P_i'\right|+\left|O\prime_i\right|\right)^2}\right] \tag{10}$$

where O_i is the index computed from ENACT data value for the ith observation, P_i is the index value computed from GCMs data for the ith observation, $\bar{O}$ is the mean of the index computed from ENACT data, and n is the number of observations, $P'_i = P_i - \bar{O}$ and $O'_i = O_i - \bar{O}$.

Changes in climate extremes in the mid and end terms of the century relative to the baseline period were computed as (Feyissa *et al.*, 2018):

$$\Delta I=\frac{I_{\text{p}}-I_{\text{b}}}{I_{\text{b}}}\times 100 \tag{11}$$

for precipitation indices and

$$\Delta I=I_{\text{p}}-I_{\text{b}} \tag{12}$$

for temperature indices, where ΔI = change in index, I_{p} = index in each period, and I_{b} = index in the baseline.

10970088, 2022, 4, Downloaded from https://rmets.onlinelibrary.wiley.com/doi/10.1002/joc.7378 by Johns Hopkins University, Wiley Online Library on [28/12/2022]. See the Terms and Conditions (https://onlinelibrary.wiley.com/terms-and-conditions) on Wiley Online Library for rules of use; OA articles are governed by the applicable Creative Commons License

The generalized extreme value (GEV) distribution was used to understand the change in the distribution of variance of some extreme indices using the following formula (Omey *et al*., 2009):

$$G(z)=\exp\left\{-\left(1+\xi\left(\frac{Z-\mu}{\delta}\right)\right)^{-1/\xi}\right\} \quad (13)$$

For $1+\xi(z-\mu)/\sigma>0$, μ = location parameter, σ = scale parameter and ξ = shape parameter.

Finally, changes in extreme values for selected indices at landscape level are interpolated from site values. Inverse distance weighting (IDW), a commonly used approach for estimation of missing data in hydrology and geographical sciences (Teegavarapu and Chandramouli, 2005), was applied using ArcMap 10.6.1. The IDW interpolated values were computed as:

$$\theta_m=\frac{\sum_{i=1}^{n}\theta_i d_{mi}^{-k}}{\sum_{i=1}^{n} d_{mi}^{-k}} \quad (14)$$

where θ_m is the observation at the location m, n is the number of stations, θ_i is the observation at station i, d_{mi} is the distance from the location of station i to location m, and k is referred to as friction distance, which can range from 1.0 to 6.0 and is fixed at 2.0 in this study.

3 | RESULTS AND DISCUSSION

3.1 | Historical extreme analysis

3.1.1 | Precipitation indices

Total precipitation and all precipitation-related extremes exhibit a significant topographic dependence across Choke Mountain. From the ENACTS data, total rainfall, rainfall intensity and number of CWD showed an increasing trend as one moves from low elevation AES (AES_1) to high elevation AES (AES_5). Meanwhile, CDD declined with increase in elevation (Figure 2). These patterns are unsurprising, and they capture the fact that AES_1 is a relatively dry, drought prone area, in which prolonged CDD are common and pose significant risks to agricultural production, while high elevation AES are wetter and more vulnerable to destructive rainfall events, snows, storms and associated erosion. Analysis of downscaled data from both MIROC5 and IPSL generally captures the spatial pattern observed with the ENACTS data at AES scale (Supplementary Table 8), as NEX-GDDP downscaling resolves the general topography of Choke Mountain.

Trends in total precipitation and precipitation extremes derived from ENACTS data indicate that rainfall amount and rainfall extremes generally decreased in Choke Mountain over the study period, with some heterogeneity across sites (Figure 2; Supplementary Table 1). At landscape level, most studied sites in western and northern parts of Choke Mountain showed statistically significant trends in prcptot unlike those located in the southern slope of the mountain (Figure 2a).

Statistically significant decreasing trends in prcptot were more prevalent in high and low elevation AES than in the middle elevations. About 40%, 22%, 25% and 46% of the sites in AES_1, AES_2, AES_3 and AES_5, respectively, showed a significant decreasing trend. Only three sites (one in AES_2 and two in AES_5) showed a significant increasing trend in prcptot (Figure 2a).

Trends in other rainfall extreme indices generally follow the pattern of total precipitation. Statistically significant trends were most prevalent for sdii, which showed a significant decreasing trend in all AES and sites except for a few in the west, southwest, east and northeast part of watersheds (Figure 2d and Supplementary Table 1). In 80%, 89%, 29% 100% and 82% of the sites, there was a significant decreasing trend of sdii in AES_1–AES_5, respectively (Supplementary Table 8). Statistically significant declines of rx5day were most prevalent for low and high elevation AES (Figure 2c), which were consistent with the pattern observed for prcptot. Results for other intensity indices (rx1day, r10mm and r20mm) generally agree with this pattern, with the greatest prevalence of statistically significant declines in low and high elevation AES. But these metrics show some heterogeneity in the sign of statistically significant trends (Figure 2b, e,f), with a few stations showing statistically significant positive trends (Supplementary Tables 1 and 8).

Collectively, the results of prcptot and rainfall intensity indices showed a picture of general drying across all of Choke Mountain with some localized heterogeneity. The results also indicate that change in rainfall extremes is most prevalent at sites located in low and high AES, which also happen to be the most climate vulnerable parts of the mountain (Simane *et al*., 2016). Agronomically, the decline in prcptot in the lower elevation AES poses a significant risk to crop production, as the area already receives relatively low rainfall, and any further reduction will bring moisture stress. This is particularly true for the beginning and end of the growing season (Frahm *et al*., 2004; Eggen *et al*., 2019). In the higher AES, the reduction in prcptot can affect agricultural water management, particularly through reducing the volume of rivers and streams that are used for small-scale irrigation during the dry season. The reduction in rainfall

10970088, 2022, 4, Downloaded from https://rmets.onlinelibrary.wiley.com/doi/10.1002/joc.7378 by Johns Hopkins University, Wiley Online Library on [28/12/2022]. See the Terms and Conditions (https://onlinelibrary.wiley.com/terms-and-conditions) on Wiley Online Library for rules of use; OA articles are governed by the applicable Creative Commons License

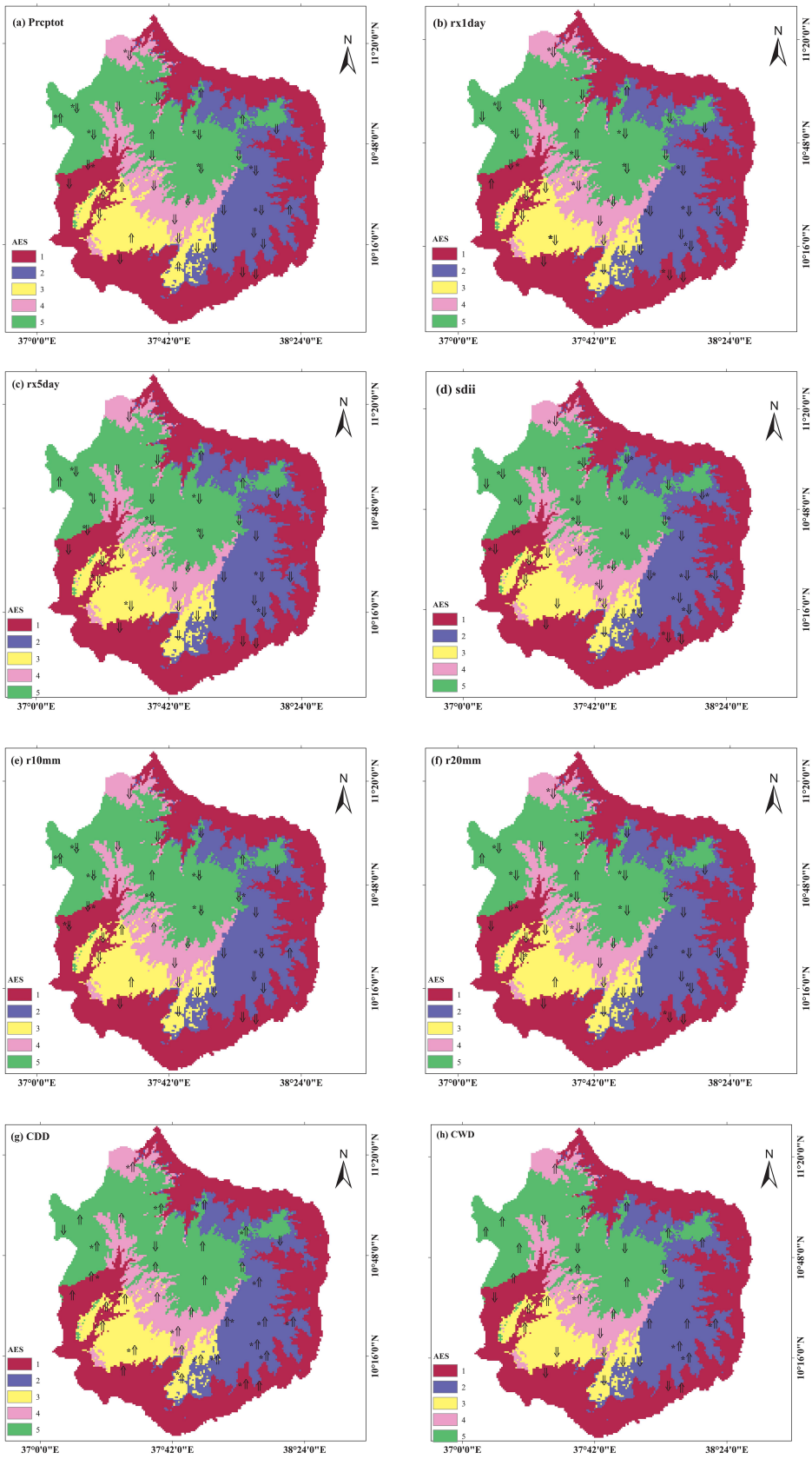

FIGURE 2 Trends of rainfall indices on Choke Mountain (1981–2016): (a) total precipitation, (b) maximum one-day precipitation, (c) maximum five-day precipitation, (d) simple daily intensity index, (e) heavy precipitation days, (f) very heavy precipitation days, (g) consecutive dry days, and (h) consecutive wet days. Downward/upward arrows represent decreasing/increasing trends, and * indicates a significant trend [Colour figure can be viewed at wileyonlinelibrary.com]

intensity (rx1day and rx5day) may have some positive impacts on soil fertility via reducing soil erosion and landslide risk. However, the reduction in prcptot in higher AES also associated with rainfall reductions at the beginning and end of the growing season poses a production risk for long season crops.

10970088, 2022, 4, Downloaded from https://rmets.onlinelibrary.wiley.com/doi/10.1002/joc.7378 by Johns Hopkins University, Wiley Online Library on [28/12/2022]. See the Terms and Conditions (https://onlinelibrary.wiley.com/terms-and-conditions) on Wiley Online Library for rules of use; OA articles are governed by the applicable Creative Commons License

TABLE 3 Trend test of CDD and CWD in the Choke Mountain Watersheds (1981–2016)

	Consecutive dry days (CDD)						Consecutive wet days (CWD)					
	Main rain season		Dry season		Small rain season		Main rain season		Dry season		Small rain season	
AES	Z	Slope	Z	Slope	Z	Slope	Z	Slope	Z	Slope	Z	Slope
1	−0.98	-0.04^{ns}	1.25	0.36^{ns}	2.47	0.44^{**}	0.76	0.05^{ns}	0.93	0.030^{ns}	2.16	0.064^{**}
2	−1.54	-0.07^{ns}	2.02	0.57^{**}	3.76	0.56^{***}	2.02	0.33^{**}	0.81	0.025^{ns}	1.81	0.053^{*}
3	−2.66	-0.09^{***}	2.56	0.67^{**}	3.24	0.53^{***}	0.95	0.12^{ns}	0.64	0.017^{ns}	0.41	0.018^{ns}
4	−2.59	-0.11^{***}	0.95	0.20^{ns}	2.47	0.43^{**}	1.06	0.17^{ns}	0.96	0.032^{ns}	0.52	0.019^{ns}
5	−1.95	-0.11^{*}	0.78	0.20^{ns}	1.93	0.25^{*}	0.99	0.19^{ns}	0.07	0.024^{ns}	0.82	0.025^{ns}

Abbreviations: AES, agroecosystem; ns, non-significant ($p > 0.1$); S, slope of the line; Z, Mann-Kendal test.
*, ** and ***significant at 10%, 5%, 1% and 0.1% probability respectively.

Trends in CWDs and CDDs reveal another aspect of precipitation change. The observed increase in CDD at most sites across AES (Figure 2g; Supplementary Table 8) is roughly consistent with the observed decreases in precipitation indices. Interestingly, however, the prevalence of statistically significant increase in CDD is greatest in AES_3, located at mid-elevation, which is the opposite of the spatial pattern of trend prevalence seen for other metrics (Figure 2g). Even more surprisingly, CWD trends, though quite mixed site-by-site (Figure 2h; Supplementary Table 1), show a tendency towards statistically significant increases, which are seen most frequently in middle elevation AES ($AES_{2–4}$). This increase in CWD in the context of declining prcptot indicates that rainy season precipitation is becoming more clustered in time, with fewer heavy rainfall days but increased number of wet days (Supplementary Figure 5).

Agronomically, these changes in CDD and CWD have several implications. The CWD result implies a shift towards more days with light rain, which is also confirmed by the analysis of the number of rainy days (Supplementary Figure 5). This has potential benefits, particularly for shallow rooted crops that are sensitive to water stress. Farmers describe such low intensity episodes as "a rain neither damages the leaf nor erodes the soil". From a management perspective, these conditions are also favourable for top dressing of additional fertilizer, but consistently muddy conditions can also interfere with other field management operations. An increase in CWD in July and August may specifically benefit Teff cultivation in AES_2, as a more frequent wet condition is required for land preparation and planting on Vertisols (heavy clay soils). Impacts of an increase in CDD depend very much on crop type and timing. An increase in CDD during the planting season can affect germination and emergence, and lead to crop failure and thereby either a need to replant or to a significant decrease in plant population and subsequent yield. However, most CDD occur in the dry season.

Considering the agricultural implications of seasonal CDD and CWD, AES level seasonal analysis was performed for these metrics. The analysis revealed that CDD in the main rain season showed a significant decreasing trend in $AES_{3–5}$, and a non-significant decreasing trend was observed in $AES_{1\ and\ 2}$ (Table 3 and Supplementary Figure 6a). $AES_{2–3}$ and all AES showed a significant increasing trend for dry and small rain seasons, respectively. An increase in CDD in dry season can facilitate harvest operations. A drastic increase in the dry season and small rain season CDD can impact base flow in streams and can also harm perennial crops, as the soil moisture falls below the permanent wilting point for long period. Moreover, the small rain season is important for planting of potato in $AES_{4\ and\ 5}$ and the long season crops like Maize and Sorghum in $AES_{1\ and\ 3}$, and the increasing trend in CDD will bring drought, which significantly affect growth and yield. An increase in CDD in December–February, however, can facilitate harvest operations. Seasonal analysis for CWD showed that only AES_2 for the main season and $AES_{1\ and\ 2}$ for the small rain season showed a significant increasing trend, and the rest seasons and AES showed insignificant positive trend (Table 3).

Results of the present study are consistent with the previous findings regardless of the spatial and temporal variations. For instance Gebrechorkos *et al.* (2019) reported the increasing and decreasing trends precipitation indices over Ethiopia, Kenya and Tanzania without any general pattern. Contrary to this, a study conducted in southwest Ethiopia reported a significant increase in R20mm (Degefu and Bewket, 2014). Another study in the central rift valley of Ethiopia showed insignificant trend change in most of the sites studied (Mekasha *et al.*, 2014). A study conducted in a similar region reported insignificant trend change in precipitation extremes (Shang *et al.*, 2011).

The ability of bias corrected and downscaled GCMs to capture characteristics of precipitation extremes was

10970088, 2022, 4, Downloaded from https://rmets.onlinelibrary.wiley.com/doi/10.1002/joc.7378 by Johns Hopkins University, Wiley Online Library on [28/12/2022]. See the Terms and Conditions (https://onlinelibrary.wiley.com/terms-and-conditions) on Wiley Online Library for rules of use; OA articles are governed by the applicable Creative Commons License

TABLE 4 Comparison of precipitation indices computed from GCMs with ENACTS dataset

GCMs	Metrics	CDD	CWD	r10mm	r20mm	rx1day	rx5day	Prcptot	Sdii
IPSL-CM5A-LR	*d*	0.66	0.25	0.48	0.96	0.49	0.38	0.98	0.5
	pbias	12	−49	31	−5	−37	−71	4	20
MIROC5	*d*	0.66	0.16	0.41	0.86	0.25	0.36	0.98	0.7
	pbias	10	39	34	−19	−113	−60	4	10

Note: *d*, Wilmot index of agreement; pbias, percentage of bias.

investigated by averaging point-wise comparison across all sites. Table 4 shows the Wilmot index of agreement (*d*) and percent bias (pbias) for indices computed from ENACTS data and from NEX-GDDP bias-corrected realizations of the IPSL and MIROC5 GCMs. Comparisons for prcptot and r20mm are quite strong, as would be expected for models that were bias corrected for total precipitation (Table 4). Results are mixed for other indices. Although NEX-GDDP includes quantile matching, the approach does not necessarily capture the frequency of very extreme events. Results of CDD are relatively good as well ($d > 0.5$, and pbias on order of 10%), perhaps because of the long dry periods that occurred in this region during the winter season. Other indices prove to be more difficult for the GCMs, even after bias correction and downscaling. For example, calculated *d* is very low (<0.5) while the percent bias is very large for most of the precipitation indices studied, such as CWD, r10mm, rx1day and rx5day (Table 4).

Interpretation of trends in GCMs over the historical period must be approached with caution. The retrospective analysis period is 36 years long, which is sufficient for many trend analyses, but calculated trends could be the product of decadal variability in addition to long-term change. As the GCM realizations used here are century scale runs that are initialized from equilibrium conditions, single realizations of a model may catch decadal variability in different phases from what was observed in the historical record. With this caveat in mind, it is still noteworthy that downscaled GCM simulation included in this study shows evidence of the reductions in total precipitation and precipitation extremes that were observed in ENACTS data (Supplementary Table 5). In most cases, the downscaled GCMs show no significant trend, and in some cases, MIROC5 shows significant increases in precipitation extremes where observations tend towards significant decreases. The only point of agreement is in CWD, where both IPSL and ENACT have statistically significant increases dominating over decreases (Supplementary Tables 5 and 8). The contrast between GCM results and ENACT observations does not disqualify these GCMs for use in future climate projection. Both have shown some performance strengths relevant to Blue Nile basin climate simulation (Bhattacharjee and Zaitchik, 2015), and as noted, 36 years is a relatively short period for model-observation trend comparisons. The absence of statistically significant trends in the downscaled GCMs, however, does point to a potential limitation in our application of GCMs to studies of extremes on this scale. While both downscaled models are able to capture extremes according to the indices used in this analysis, albeit with some substantial bias relative to observations (Supplementary Table 8), the downscaling approach is stationary in time. Insomuch as trends in extremes might be influenced by shifts in local dynamics in response to a large-scale climate change forcing (i.e., locally nonstationary dynamics); the downscaled GCM outputs used in this study will miss some dynamics of local change.

3.1.2 | Temperature indices

Compared with precipitation indices, temperature indices and trends are more coherent in observations and consistent between observations and models. The distribution of mean values of all extreme indices follow expected elevation gradients. SU25 is highest in AES_1 and lowest in AES_5, with annual increasing by 1.43–2.8 and 0.99–2.51 days/year, respectively. In contrast, FD10 is highest in AES_5 (201 days with a reduction of 2.01–3.7 days/year) and lowest in AES_1 (reduced by 1.22–2.62 days/year). All TXx, TXn, TNx and TNn show highest mean values in AES_1 and lowest mean values in AES_5 (Figure 3 and Supplementary Tables 2 and 9).

A general warming in recent decades is observed, which resulted in positive trends in SU25, TXx, TXn, TNx, TNn, TX90P and TN10P, while FD10, TX10P and TN10P showed a decreasing trend, with some spatial variability in the significance of trends (Figures 3 and 4 and Supplementary Tables 2 and 3). DTR showed both significant increasing and decreasing trends for sties in AES_{1-3} and a significant increasing trend in AES_{4-5} (Supplementary Table 4 and Figure 4e). Between the GCMs, MIROC5 showed a significant decreasing trend in all AES, and IPSL showed insignificant trend in all AES. In general, a higher significant trend in temperature extremes is observed in higher elevation AES (Figure 3 and

10970088, 2022, 4, Downloaded from https://rmets.onlinelibrary.wiley.com/doi/10.1002/joc.7378 by Johns Hopkins University, Wiley Online Library on [28/12/2022]. See the Terms and Conditions (https://onlinelibrary.wiley.com/terms-and-conditions) on Wiley Online Library for rules of use; OA articles are governed by the applicable Creative Commons License

Supplementary Table 2). The magnitude of these trends differs substantially by location and AES (Figures 3 and 4 and Supplementary Tables 2 and 3).

TNn in some sites (19%) showed a decreasing trend that reflects an increase in temperature variance, which can cause an increase in extreme cold events despite of

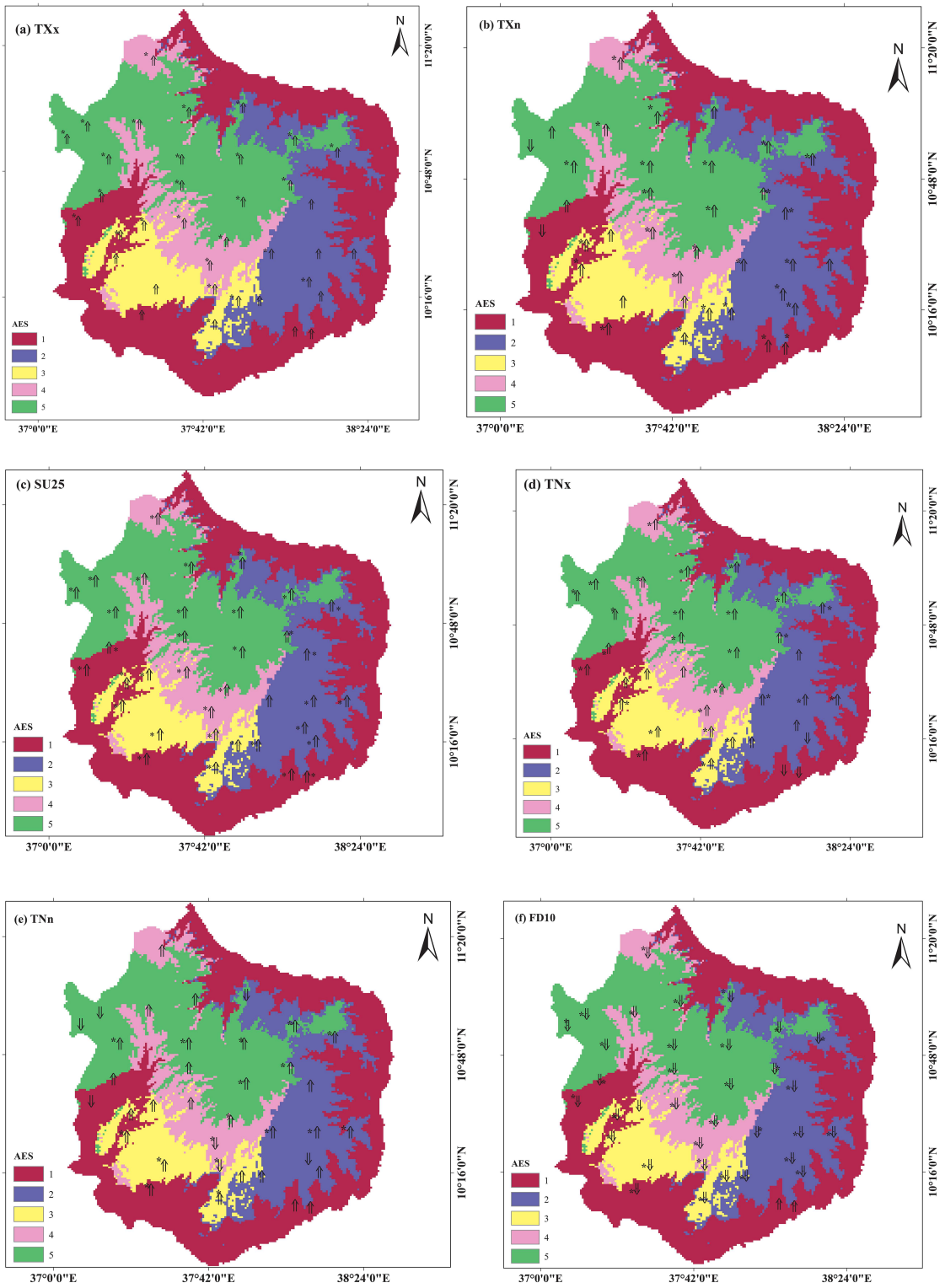

FIGURE 3 Trends of temperature indices in Choke Mountain (1981–2016): (a) TXx, (b) TXn, (c) SU25, (d) TNn, (e) TNx, and (f) FD10. Downward/upward arrows represent decreasing/increasing trends, and * indicates a significant trend [Colour figure can be viewed at wileyonlinelibrary.com]

10970088, 2022, 4, Downloaded from https://rmets.onlinelibrary.wiley.com/doi/10.1002/joc.7378 by Johns Hopkins University, Wiley Online Library on [28/12/2022]. See the Terms and Conditions (https://onlinelibrary.wiley.com/terms-and-conditions) on Wiley Online Library for rules of use; OA articles are governed by the applicable Creative Commons License

increases in mean temperature (Anav *et al.*, 2010; Medvigy *et al.*, 2012).

The ability of downscaled GCMs to reproduce temperature indices is better than precipitation indices in most cases (Table 5). This is consistent with the general understanding that temperature, a smoothly varying field for which underlying physical processes are relatively well understood, is better captured by GCMs. This could

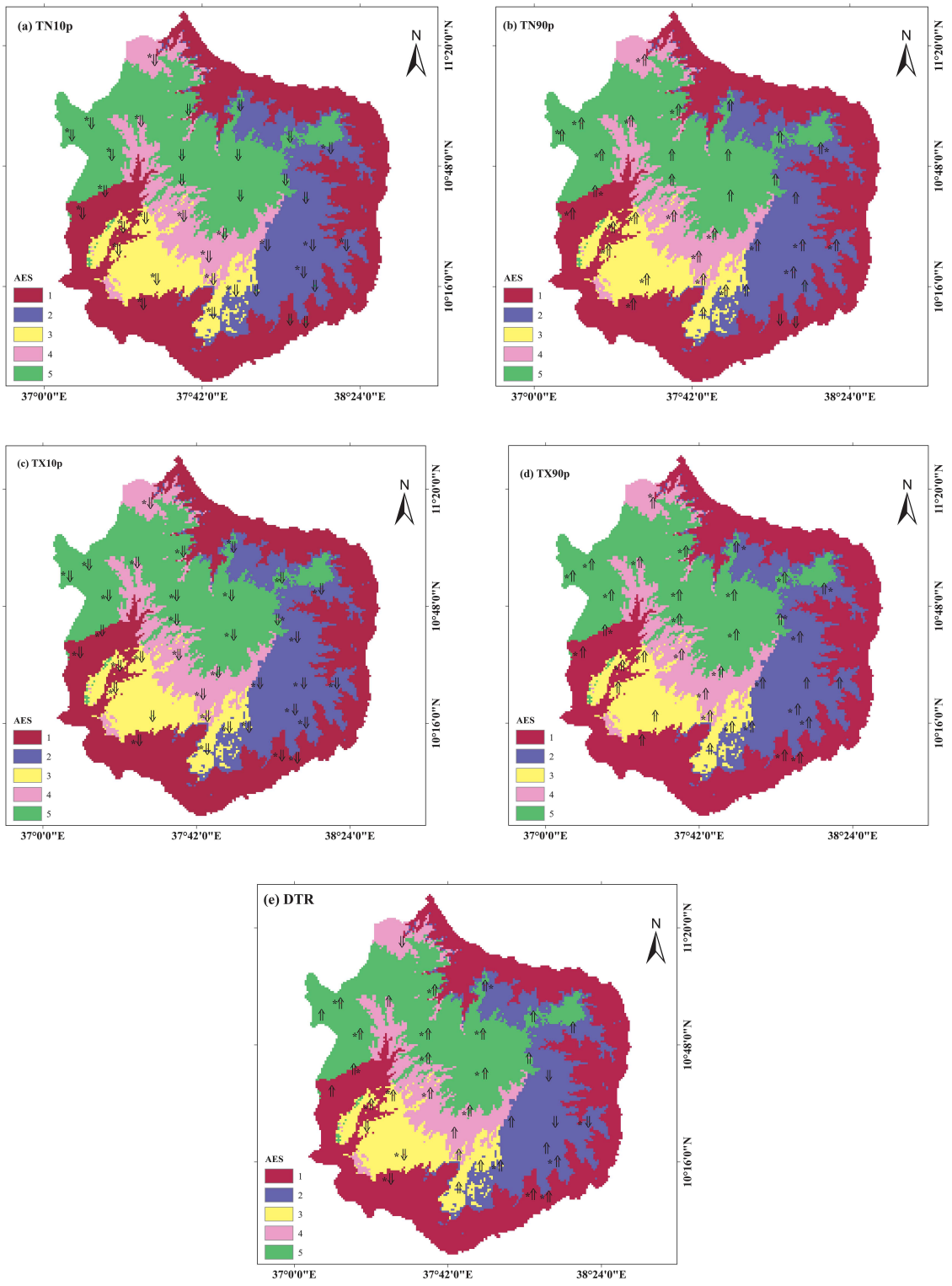

FIGURE 4 Trends of temperature indices in Choke Mountain (1981–2016): (a) TN10P, (b) TN90P, (c) TX10P, (d) TX90P, and (e) DTR. Downward/upward arrows represent decreasing/increasing trends, and * indicates a significant trend [Colour figure can be viewed at wileyonlinelibrary.com]

10970088, 2022, 4, Downloaded from https://rmets.onlinelibrary.wiley.com/doi/10.1002/joc.7378 by Johns Hopkins University, Wiley Online Library on [28/12/2022]. See the Terms and Conditions (https://onlinelibrary.wiley.com/terms-and-conditions) on Wiley Online Library for rules of use; OA articles are governed by the applicable Creative Commons License

TABLE 5 Comparison of temperature indices computed from GCMs with ENACT dataset

GCMs	Metrics	SU25	FD10	TXx	TXn	TNn	TNx	TX10p	TX90p	TN10p	TN90p	DTR
IPSL-CM5A-LR	*d*	0.91	0.81	0.99	0.99	0.46	1	0.18	0.2	0.14	0.2	0.59
	pbias	14	−39	0	0	17	0	3	−5	−1.7	−2	3
MIROC5	*d*	0.92	0.85	0.93	0.87	0.15	0.98	0.17	0.12	0.17	0	0.4
	pbias	19	−37	−3	4	37	2	5	−3	0.1	−0.3	25

Note: *d*, Wilmot index of agreement; pbias, percentage of bias.

be because precipitation exhibits high spatial and temporal variations that cannot be captured by GCMs.

While TXx, TXn and TNx are quite well captured by the GCMs, however, there are substantial biases for SU25 and FD10, which are both threshold indices, and TX10P, TX90P, TN10P and TN90P, which are percentile indices, and DTR, which is sensitive to even modest bias in GCM representation of temporal variability in temperatures. In this case, both GCMs have a positive bias for SU25, TN90P and TX90P and a negative bias for FD10, TX10P, TX90P and DTR, suggesting that the bias correction and downscaling process overestimates the warm tail and underestimates the cold tail of the temperature distribution relative to ENACTS data. Interestingly, TNn and DTR show significant positive bias in both GCMs. This is consistent with the FD10 result, and it suggests that the downscaled GCMs have a particular problem capturing cold extremes in this region.

For temperature trends, GCMs generally reproduce the positive trends observed in ENACTS data (Supplementary Table 5), albeit with less ability to capture AES-level variability in the prevalence of statistically significant trends. This lack of spatial structure in trends indicates that the GCMs do not resolve processes relevant to differing warming trends across Choke's elevation gradient. Downscaling can bring the models into agreement with observations for the spatial structure of mean values in temperature extremes (Table 5), but the BCSD downscaling method cannot introduce nonstationary processes that are not resolved by GCMs. This fact should be kept in mind when applying downscaled GCM analyses to studies of climate trends and vulnerabilities. Over the period of analysis MIROC5 shows fewer significant trends than IPSL, indicating that this realization of MIROC5 had a lower overall warming trend than IPSL for this region.

Trends in temperature indices could have significant implications for crop production in the region. The decrease in FD10 in high elevation areas will significantly hinder the production of cool season crops, such as apples, which require cold days to initiate flower buds via vernalization, and hence, their orchards will face reduction of yield or increase of non-viability as the number of FD10 days drops. On the other hand, reduction in the risk of frost and other cold damage could benefit agriculture by extending growing seasons and allowing for introduction of cold-sensitive plants higher on the mountain. The increase in temperature in higher AES will also hasten plant growth, potentially allowing for double crop cultivation in a year. The increase in SU25 in lower elevation AES will bring a challenge for crop production, as the higher temperature causes heat stress coupled with an increase in evapotranspiration and moisture stress.

Results of the present study are consistence with the findings of previous studies. A study conducted in east African region showed that warm days and nights, warm spell duration indicator and summer days showed a significant increasing trend, whereas cold days and nights showed a significant decreasing trend (Gebrechorkos *et al*., 2019). Another study conducted in the central rift valley of Ethiopia showed a significant increasing trend for warm indicators and a significant decreasing trend for cold-related indices (Mekasha *et al*., 2014). A study conducted in southern Ethiopia also showed a significant increasing trend in both warm and cold indicator indices in high and low altitude areas unlike the mid-altitude areas (Esayas *et al*., 2018a).

3.2 | Future extreme analysis

3.2.1 | Projected change in precipitation indices

The ability of selected GCMs to reproduce precipitation indices in the historical period is shown in Table 4, and only indices showing strong agreement with ENACTS dataset indices are selected for the projected period. The primary result from downscaled projections of future precipitation extremes is that both models project wetting across Choke Mountain over the 21st century (Figure 5; Supplementary Table 3; Supplementary Figure 7).

Interestingly, for total precipitation and very heavy precipitation days, MIROC5 (Figure 5b,d) shows somewhat stronger trends than IPSL (Figure 5a,c), particularly for mid-century and moderate emissions (RCP4.5-M). This contrasts with the fact that IPSL has stronger temperature trends in the retrospective period and, as will be discussed later, in its projections. For the case of these

10970088, 2022, 4, Downloaded from https://rmets.onlinelibrary.wiley.com/doi/10.1002/joc.7378 by Johns Hopkins University, Wiley Online Library on [28/12/2022]. See the Terms and Conditions (https://onlinelibrary.wiley.com/terms-and-conditions) on Wiley Online Library for rules of use; OA articles are governed by the applicable Creative Commons License

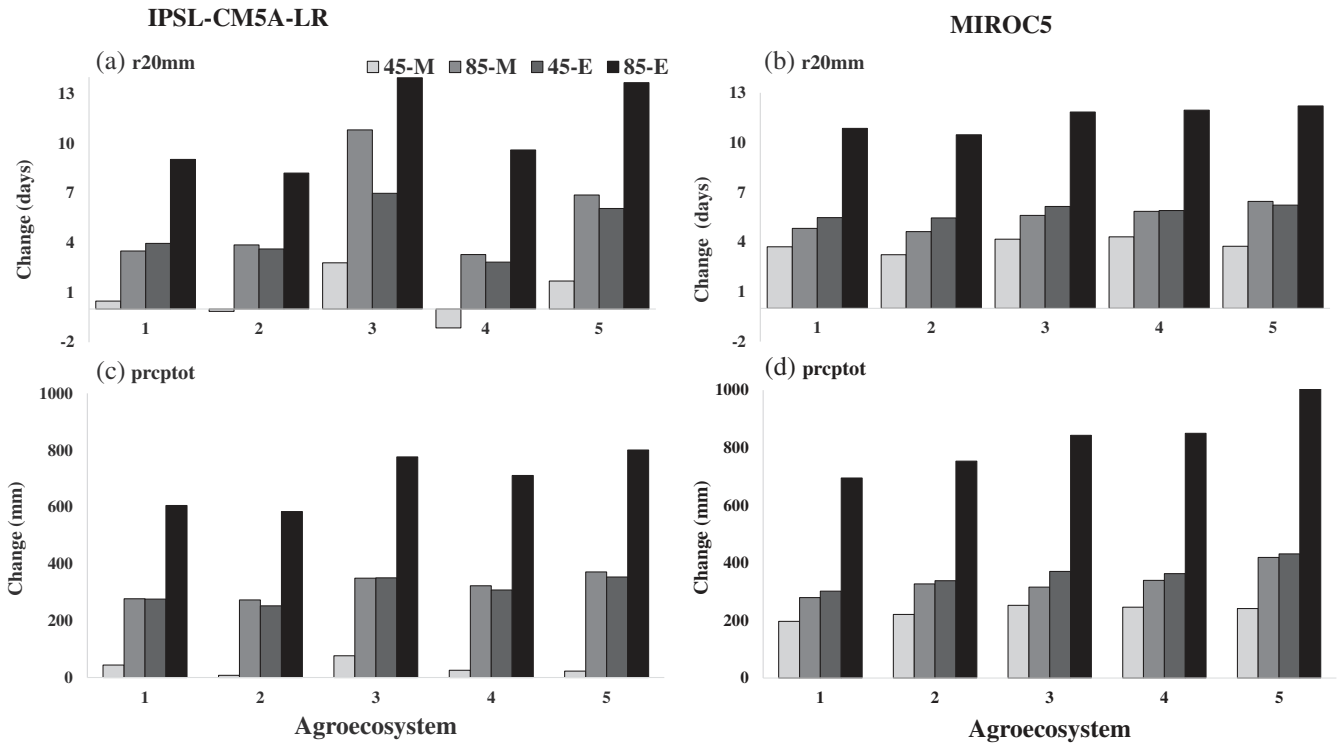

FIGURE 5 Projected changes in very heavy precipitation days (a,b) and total precipitation (c,d) in the mid and end of the 21st century. Projections are given for mid (M) and end (E) of the 21st century periods, for RCPs 4.5 and 8.5. See Supplementary Table 3 for precise numbers

two model realizations, then, change in precipitation extremes does not scale with change in temperature. As expected, changes are larger for the high emissions scenario (RCP8.5) and later in the 21st century (end [E] vs. middle [M] in Figure 5).

The results show relatively little contrast between AES, though trends are slightly stronger for higher elevation AES in most cases. Contrasts between AES in these downscaled GCM projections, however, may be overly smoothed. As noted previously, the downscaling technique cannot capture non-stationarity that is not resolved by the GCM. In addition, these projections do not account for any local land surface changes, including land cover conversions, that might contribute to local climate changes. In keeping with these AES-averaged projections, reasonably strong consistency was observed in total precipitation trends across the studied sites (Supplementary Figure 1). There is site-to-site variability in the magnitude of trends, and spatially interpolated projections show some spatial structure (Supplementary Figure 1), but aside from an elevation effect, these spatial patterns are not particularly systematic or consistent across time periods, scenarios or GCMs.

3.2.2 | Change in temperature indices

Projected temperature trends were relatively consistent across models, where both models showed a warming and an increase in extremes (but decrease in FD10) that rises from mid-21st century to late-21st century and is highest in the late-21st century for RCP8.5 (Figure 6; Supplementary Table 7). For the mid-21st century period, there is relatively little difference between emissions pathways, which is consistent with the understanding that these trajectories diverge primarily in the second half of the 21st century.

Projected changes are generally uniform across different AESs for the minimum and maximum temperature indices, but there is spatial structure for the threshold indices (FD10 and SU25). For both, the change in number of days is projected to be smallest in AES_1 than it is in other AES, reflecting the fact that this low-lying AES already has relatively few FD10 days and a large number of SU25 days (Figure 6). There is also a tendency towards stronger trends on the eastern side of the mountain and smaller trends for the southern and western slopes (Supplementary Figure 2). This pattern warrants further investigation. Choke Mountain is located at the intersection of multiple atmospheric circulations, including westerly winds associated with the Congo Air Stream and south-easterly flow in from the Indian Ocean. Zonal structure to projected climate trends could reflect shifting influence of different airmasses or differences in trends within those airmasses.

The IPSL simulation projects more dramatic trends than MIROC5 for all indices except TXx (Figure 6). This

10970088, 2022, 4, Downloaded from https://rmets.onlinelibrary.wiley.com/doi/10.1002/joc.7378 by Johns Hopkins University, Wiley Online Library on [28/12/2022]. See the Terms and Conditions (https://onlinelibrary.wiley.com/terms-and-conditions) on Wiley Online Library for rules of use; OA articles are governed by the applicable Creative Commons License

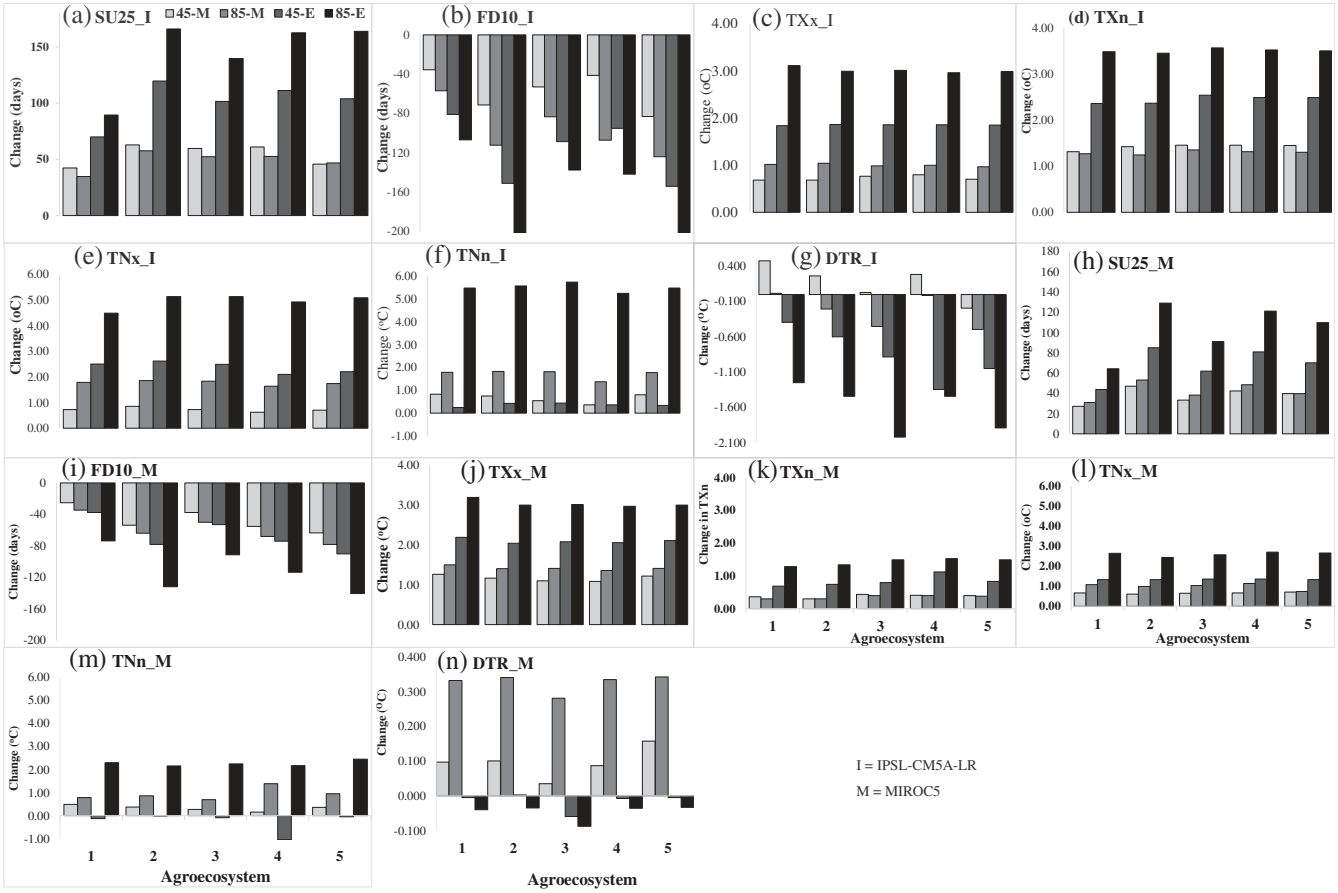

FIGURE 6 (a-n) Change in temperature indices in the mid and end of the 21st century

is consistent with trends over the historical period (Supplementary Table 4), in which IPSL showed more sensitivity than MIROC5. The TXx result indicates that the MIROC5 simulation still produces some extremely hot days, although the other elements of the temperature distribution shift more modestly than they do in IPSL (Figure 6c,j).

Importantly, the prospective temperature extreme analysis showed that the future changes in climate extreme indices are not only a simple mean shift, but also a change in the shape of distribution and the variance. The variance for mean minimum and maximum temperature is presented in Figure 7. For MIROC5, maximum temperature variance increases consistently from baseline to mid-21st century to late-21st century (Figure 7, left top), while minimum temperature variance is relatively flat in baseline to mid-21st century before increasing in late-21st century (Figure 7, left bottom).

For IPSL, minimum temperature also shows a steady increase in variance from baseline to mid-21st century to late-21st century (Figure 7, right bottom), but the IPSL maximum temperature result is not consistent. The variance of mean maximum temperature decreased in the mid-21st century and then increased in late-21st century (Figure 7, right top). As this is the result of a single realization, the unexpected variance result in the mid-21st century for IPSL could be a result of decadal variability in that model realization. Analysis of a larger ensemble of realizations would be required to determine whether this signal is meaningful. A change in the variance can have a larger effect on the frequency and intensity of extremes than a change in the mean (Katz and Brown, 1992).

Supplementary Figures 3 and 4 show the generalized extreme value (GEV) PDF for mean maximum and minimum temperatures obtained from the two GCMs under RCP8.5. As shown in the figures, the distribution of values and the mean both change with time. For instance, the mean and variance of maximum temperature at AES1 (Supplementary Figure 3, left top) shifted by 1.06°C and 3.43°C, and −0.25 and 0.13 for IPSL and 1.90°C and 5.13°C, and 0.19 and 0.31 for MIROC5 in the mid and end period, respectively (Figure 7, left top, and Figure 7, right top).

There are also higher order shifts in distribution projected over the 21st century. The kurtosis of the PDF curve for maximum and minimum temperature, for

10970088, 2022, 4, Downloaded from https://rmets.onlinelibrary.wiley.com/doi/10.1002/joc.7378 by Johns Hopkins University, Wiley Online Library on [28/12/2022]. See the Terms and Conditions (https://onlinelibrary.wiley.com/terms-and-conditions) on Wiley Online Library for rules of use; OA articles are governed by the applicable Creative Commons License

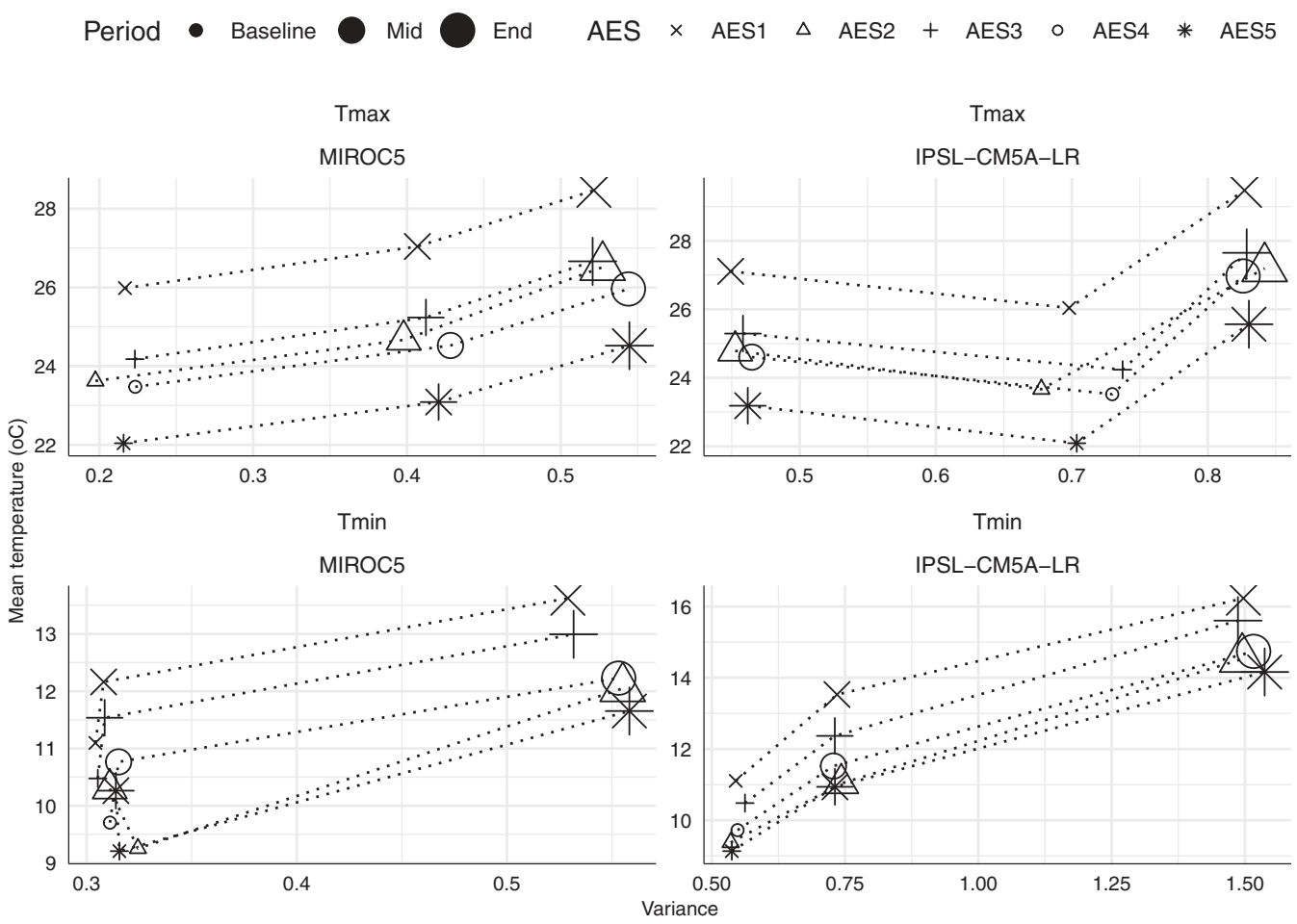

FIGURE 7 Distribution of mean maximum and minimum temperature variance in the Choke Mountain watersheds

example, shows variable changes through mid-century, but by late-21st century, there is a tendency towards platykurtic distributions—generally flatter around the mean, though with fewer extreme outliers relative to the variance—that is indicative of an increase invariability (Supplementary Figures 3 and 4).

3.2.3 | Complexity of agricultural impacts of projected extremes

Many of the agronomic implications of projected changes in temperature extremes can be viewed as intensified extensions of impacts related to current warming trends. Thus, the risks to temperate crops at high elevation and heat and drought sensitive crops at low elevation of the mountain will increase, while growing season length may extend at high elevation AES. Some implications of projections, however, are qualitatively different from those of the moderate warming observed in recent decades. For example, high temperatures in low elevation AES are projected to exceed the maximum heat tolerance of some currently grown crops, suggesting that appropriate adaptation activities are required if agriculture is to remain viable in these areas. Some of the viable adaptation options in the lowland areas could be in situ water harvesting activities that can reduce heat and moisture stress, implementation of agroforestry practices to modify the microclimate, working on genetic improvements for heat and drought tolerance and crop switching. In addition to crop switching, significant management changes might be required regarding irrigation availability and frequency, control of newly emerging pests and the type and timing of fertilizer application. These new challenges carry implications for costs, resources and infrastructure.

Choke Mountain experienced a decrease in precipitation extreme indices and an increase in temperature extreme indices in the baseline period. The increase in temperature in projected periods resulted in a smaller number of FD10, which has negative implications for the expansion and productivity of some perennial crops originated in the temperate region, such as apples. Temperate

10970088, 2022, 4, Downloaded from https://rmets.onlinelibrary.wiley.com/doi/10.1002/joc.7378 by Johns Hopkins University, Wiley Online Library on [28/12/2022]. See the Terms and Conditions (https://onlinelibrary.wiley.com/terms-and-conditions) on Wiley Online Library for rules of use; OA articles are governed by the applicable Creative Commons License

crops (including fruit trees and grape vines) require exposure to some numbers of chilling hours, and with rising temperatures, chilling hours will be reduced (Hatfield *et al*., 2014). The positive change in TXx, SU25, TXn, TNx and TNn would also result in negative effects on crop production due to its influence on physiological processes, resource utilization and water productivity. Relatively few adaptation strategies are available to cope with this situation; changes in crop selection could be the most effective response.

The reduction in DTR reflects the fact that the minimum daily temperature is projected to increase at a higher rate than the maximum. This would affect temperature dependent basic plant processes (photosynthesis, dry matter production and dry matter partitioning) and developmental processes. For example, tuber initiation in potato, one of the major crops in the Choke Mountain, depends on many biological processes, including carbon partitioning, signal transduction and meristem determination, which, in turn, is affected by DTR. Low temperature promotes high C:N ratio and accumulation of more dry matter at the tip of the stolen and promotes tuber initiation (Vreugdenhil *et al*., 2007). Research also indicates that high night temperature during tuber initiation delays tuber development, thus altering tuber mass distribution by reducing the yield proportion of large tubers and lowering early harvest index, causing a significant yield loss without interfering with photosynthesis (Kim and Lee, 2019). Diurnal temperature variation is of particular importance in many orchards in the development of secondary metabolites and production of high acid and high sugar content as fruits' exposure to sunlight increases ripening qualities while the sudden drop in temperature at night preserves the balance of natural acids in the fruit (Cohen *et al*., 2012). Projected reduction in DTR could also affect the yield and quality of crops grown in the watershed. Wider DTR also had significantly positive effect on seed germination (Liu *et al*., 2013) and distribution of plant species (Rosbakh and Poschlod, 2015).

Several specific agronomic implications of trending precipitation and temperature extremes have been noted above. At the same time, it must be recognized that plant response to climate change depends on complex interactions between climate elements and between climate and human activity. As temperatures increase over this century, crop production areas may shift to the optimal temperature range that is favourable for growth and yield (Hatfield *et al*., 2011). There is an extensive literature that demonstrates how extremes of temperature and precipitation affect crop productivity in various climatic and agricultural contexts. This includes work on the impacts of temperature extremes on plant productivity (Craufurd and Wheeler, 2009; Hatfield and Prueger, 2015) and on pollen viability, fertilization and grain or fruit formation (Hatfield *et al*., 2014; Zhao *et al*., 2017). Increased variation in precipitation, coupled with shifting patterns of precipitation within the season will create more variation in soil water availability, with potentially significant impacts for crop yields (Hatfield *et al*., 2014). Such impacts are, however, location and crop specific, such that generalizing impacts of extremes on crop production from one region to another—or, for the tropical highlands, even from one AES to another—can be misleading. Crops have cardinal temperature ranges (Hatfield *et al*., 2011; Hatfield and Prueger, 2015), and any shift in the location of means and the distribution of the cardinal temperature would affect growth, development, yield and quality of crops either directly or indirectly through creating favourable conditions for pest development and distributions (Hatfield *et al*., 2014). Increasing temperatures generally cause cultivated plants to grow and mature more quickly, and if the soil is not able to supply nutrients at required rates for faster growing plants, then yield may be smaller, which may, in turn, result in reduced grain, forage, fruit or fibre production (Hatfield et al., 2014).

Further increases in temperature and changes in precipitation patterns will induce new conditions that will affect insect populations, incidence of pathogens and the geographic distribution of insects and diseases (Hatfield *et al*., 2014; Patterson *et al*., 1999). Higher winter temperatures increase insect populations due to overwinter survival, while higher summer temperatures increase their reproduction rates and allow for multiple generations in each year (Ziska and Runion, 2007; Hatfield *et al*., 2014). Moreover, the high number of very heavy precipitation days (r20mm) and more total precipitation in the projection period would also impact planning of soil and water conservation activities, infrastructure development and farm management practices.

In general, in the present study, we note that different AESs exhibit unique climate extremes that necessitate proper identification and implementation of adaptation options to maintain the sustainability of various systems. Neither ENACTS nor GCMs dataset captured a frequently occurring frost in the watershed. Moreover, GCMs did not exactly capture the precipitation extreme indices at the watershed level thought the impacts of these extremes practically noticeable. Thus, further works should be done to improve the predictability precipitation extremes from GCM datasets. However, results of the present analysis can be applicable in different parts of Ethiopia and other regions, because there are many watersheds with the same AES setup like our study region in many parts of Ethiopia and other regions.

10970088, 2022, 4, Downloaded from https://rmets.onlinelibrary.wiley.com/doi/10.1002/joc.7378 by Johns Hopkins University, Wiley Online Library on [28/12/2022]. See the Terms and Conditions (https://onlinelibrary.wiley.com/terms-and-conditions) on Wiley Online Library for rules of use; OA articles are governed by the applicable Creative Commons License

4 | CONCLUSION

Results of the present analysis indicate that precipitation indices showed decreasing trends in the baseline period in observations, while downscaled GCMs project an increasing trend in the mid and end of the 21st century. Temperature indices showed an increasing trend in observations and in both retrospective and prospective periods under both GCMs and RCPs, with few exceptions. There is site-to-site variability in these results but aggregating by the AES offers a way to characterize these trends at an agronomically relevant unit.

Projected increases in precipitation indices in the future periods, should they prove to be correct, and may have both positive and negative implications for agricultural practices and crop production in the area. The torrential rain indicated by high r20mm will bring more soil erosion, flooding and waterlogging in the area, which will affect crop performance, growth and development. It may also cause landslide and gully formation in sloping AES like AES_1, AES_4 and AES_5 that could pose significant risks for agricultural lands, crops and households in general unless drainages and waterways are properly designed and constructed.

Projected changes in temperature extremes, in which we might have greater confidence on account of stronger GCM performance in the historical period, are also critical to cropping systems. The reduction in the number of FD10 also will create ecological alterations and currently grown crops, particularly in higher elevated AES ($AES_{4–5}$), will not be viable unless due care is taken in the selection and introduction of low chilling requiring varieties. The significant increase in hot/summer days will also challenge crop production, particularly in hot dry AES (AES_1–AES_3) because of the already high temperature. The decrease in DTR will affect the quality of many fruit trees (like apple and orange trees) grown in the area and tuber and bulb formation in root (example potato) and bulb (example shallot) crops grown in the watershed. Additional warming threatens to bring the temperature above the upper threshold limit for currently growing crops. Warming will also increase potential evapotranspiration and reduce water productivity, exacerbating competition for water during the dry season.

In assessing the reliability of GCM projections, both GCMs generally agree with observations for trends in temperature extremes in the historical period. However, they generally do not match observed trends for precipitation extremes. While this can be forgiven for single realizations over a relatively short baseline period, the result bears some resemblance to the "East Africa Paradox" that has been debated for East African spring rains. There is the possibility, then, that models are systematically biased in representation of precipitation trends in this region. At the same time, the general projection that humid tropical areas like Choke Mountain are expected to wet under global warming has a meaningful theoretical foundation (as embodied in models). So, the possibility that recent drying trends are ephemeral and will reverse in future decades cannot be discounted. Agricultural adaptation planning in this region will benefit from continued efforts to understand recent trends and to improve GCM simulation of precipitation variability. In conclusion, more research in prediction of rainfall is required, and GCM for rainfall predictions shall be refuted by having more observed data across the East Africa region including the study area.

ACKNOWLEDGEMENTS

The first author was supported by the Belmont Forum Collaborative Research (NILE-NEXUS—a project award number 1624335) funded by the National Science Foundation (NSF). The authors wish to acknowledge the Ethiopian National Meteorological Services Agency (NMA) for providing data used in this study. The CCl/WCRP/JCOMM Expert Team on Climate Change Detection and Indices (ETCCDI) is also acknowledged for the provision of access to the RHtestsV3 and RHtests_dlyPrcp software packages used for homogeneity test and change point detection and for their technical comments. Department of Earth and Planetary Sciences, Johns Hopkins University, is also acknowledged for hosting the first author as a visiting student.

CONFLICT OF INTEREST

The authors have read and understood the policy on declaration of interests and declare that they have no competing interests.

AUTHOR CONTRIBUTIONS

Dereje Ademe Birhan: Conceptualization; data curation; formal analysis; investigation; methodology; validation; visualization; writing – original draft; writing – review and editing. **Benjamin F. Zaitchik:** Conceptualization; data curation; formal analysis; funding acquisition; investigation; methodology; project administration; resources; software; supervision; validation; visualization; writing – original draft; writing – review and editing. **Kindie Tesfaye Fantaye:** Methodology; supervision; validation; visualization; writing – original draft; writing – review and editing. **Belay Simane Birhanu:** Conceptualization; formal analysis; funding acquisition; methodology; project administration; validation; writing – original draft; writing – review and editing. **Getachew Alemayehu Damot:** Formal analysis; investigation; methodology; supervision; writing – original draft; writing –

10970088, 2022, 4, Downloaded from https://rmets.onlinelibrary.wiley.com/doi/10.1002/joc.7378 by Johns Hopkins University, Wiley Online Library on [28/12/2022]. See the Terms and Conditions (https://onlinelibrary.wiley.com/terms-and-conditions) on Wiley Online Library for rules of use; OA articles are governed by the applicable Creative Commons License

review and editing. **Enyew Adgo Tsegaye:** Conceptualization; formal analysis; investigation; methodology; validation; visualization; writing – original draft; writing – review and editing.

ORCID

Dereje Ademe Birhan https://orcid.org/0000-0002-0987-464X

REFERENCES

Abatan, A.A., Abiodun, B.J., Gutowski, W.J. and Rasaq-Balogun, S. O. (2018) Trends and variability in absolute indices of temperature extremes over Nigeria: linkage with NAO. *International Journal of Climatology*, 38(2), 593–612. https://doi.org/10.1002/joc.5196.

Alemayehu, A. and Bewket, W. (2017) Local spatiotemporal variability and trends in rainfall and temperature in the central highlands of Ethiopia. *Geografiska Annaler, Series A: Physical Geography*, Taylor & Francis, 99(2), 85–101. https://doi.org/10.1080/04353676.2017.1289460.

Anav, A., Ruti, P.M., Artale, V. and Valentini, R. (2010) Modelling the effects of land-cover changes on surface climate in the Mediterranean region. *Climate Research*, 41(2), 91–104. https://doi.org/10.3354/cr00841.

Atkinson, C.J., Brennan, R.M. and Jones, H.G. (2013) Declining chilling and its impact on temperate perennial crops. *Environmental and Experimental Botany* Elsevier B.V, 91, 48–62. https://doi.org/10.1016/j.envexpbot.2013.02.004.

Berg, P., Feldmann, H. and Panitz, H. (2012) Bias correction of high resolution regional climate model data. *Journal of Hydrology*. Elsevier B.V, 448–449, 80–92. https://doi.org/10.1016/j.jhydrol.2012.04.026.

Bhattacharjee, P.S. and Zaitchik, B.F. (2015) Perspectives on CMIP5 model performance in the Nile River headwaters regions. *International Journal of Climatology*, 35(14), 4262–4275. https://doi.org/10.1002/joc.4284.

Block, P.J., Strzepek, K., Rosegrant, M.W. and Diao, X. (2008) Impacts of considering climate variability on investment decisions in Ethiopia. *Agricultural Economics*, 39(2), 171–181. https://doi.org/10.1111/j.1574-0862.2008.00322.x.

Cannon, A.J. (2018) Multivariate quantile mapping bias correction: an N - dimensional probability density function transform for climate model simulations of multiple variables. *Climate Dynamics*. Springer Berlin Heidelberg, 50(1), 31–49. https://doi.org/10.1007/s00382-017-3580-6.

Cohen, S.D., Tarara, J.M., Gambetta, G.A., Matthews, M.A. and Kennedy, J.A. (2012) Impact of diurnal temperature variation on grape berry development, proanthocyanidin accumulation, and the expression of flavonoid pathway genes, 63(7), 2655–2665. https://doi.org/10.1093/jxb/err449.

Conway, G.R. (1985) Agro-ecosystem analysis. *Agriculture Administration*, 20, 31–55. https://doi.org/10.1016/0309-586X(85)90064-0.

Craufurd, P.Q. and Wheeler, T.R. (2009) Climate change and the flowering time of annual crops. *Journal of Experimental Botany*, 60(9), 2529–2539. https://doi.org/10.1093/jxb/erp196.

de los Milagros Skansi, M., Brunet, M., Sigró, J., Aguilar, E. and Jones, P.D. (2013) Warming and wetting signals emerging from analysis of changes in climate extreme indices over South America. *Global and Planetary Change*. Elsevier B.V, 100, 295–307. https://doi.org/10.1016/j.gloplacha.2012.11.004.

Degefu, M.A. and Bewket, W. (2014) Variability and trends in rainfall amount and extreme event indices in the Omo-Ghibe River basin, Ethiopia. *Regional Environmental Change*, 14(2), 799–810. https://doi.org/10.1007/s10113-013-0538-z.

Dinku, T., Cousin, R., Corral, J., Ceccato, P. and Vadillo, A. (2016) The ENACTS approach: transforming climate services in Africa one country at a time. 1–24. http://worldpolicy.org/wp-content/uploads/2016/03/The-ENACTS-Approach-Transforming-Climate-Services-in-Africa-One-Country-at-a-Time.pdf

Dinku, T., Hailemariam, K., Maidment, R., Tarnavsky, E. and Connor, S. (2014) Combined use of satellite estimates and rain gauge observations to generate high-quality historical rainfall time series over Ethiopia. *International Journal of Climatology*, 34(7), 2489–2504. https://doi.org/10.1002/joc.3855.

Eggen, M., Ozdogan, M., Zaitchik, B., Ademe, D. and Simane, B. (2019) Vulnerability of sorghum production to extreme, subseasonal weather under climate change. *Environmental Research Letters*, 14(4), 1–11. https://doi.org/10.1088/1748-9326/aafe19.

Esayas, B., Simane, B., Teferi, E., Ongoma, V. and Tefera, N. (2018a) Trends in extreme climate events over three agroecological zones of southern Ethiopia. *Advances in Meteorology*, 2018(October), 1–17. https://doi.org/10.1155/2018/7354157.

Fetene, A., Alem, D. and Mamo, Y. (2014) Effects of landuse and land cover changes on the extent and distribution of afroalpine vegetation of northern western Ethiopia: the case of Choke Mountains. *Research Journal of Environmental Sciences*, 8(1), 17–28. https://doi.org/10.3923/rjes.2014.17.28.

Feyissa, G., Zeleke, G., Bewket, W. and Gebremariam, E. (2018) Downscaling of future temperature and precipitation extremes in Addis Ababa under climate change. *Climate*, 6(3), 1–19. https://doi.org/10.3390/cli6030058.

Frahm, M.A., Rosas, J.C., Mayek-Pérez, N., López-Salinas, E. and Kelly, J.D. (2004) Breeding beans for resistance to terminal drought in the lowland tropics. *Euphytica*, 136(2), 223–232. https://doi.org/10.1023/B:euph.0000030671.03694.bb.

Gebrechorkos, S.H., Hülsmann, S. and Bernhofer, C. (2019) Changes in temperature and precipitation extremes in Ethiopia, Kenya, and Tanzania. *International Journal of Climatology*, 39(1), 18–30. https://doi.org/10.1002/joc.5777.

Gessesse, A.A., and Melesse, A.M. (2018) Decadal dynamics of land use/land cover in the Muga Watershed, Choke Mountain Range, Upper Blue Nile Basin, Ethiopia. 1–13. https://doi.org/10.20944/preprints201805.0262.v1.

Gilbert, R.O. (1987) *Statistical Methods for Environmental Pollution Monitoring*. New York, NY: VNR.

Gocic, M. and Trajkovic, S. (2013) Analysis of changes in meteorological variables using Mann-Kendall and Sen's slope estimator statistical tests in Serbia. *Global and Planetary Change*. Elsevier B.V, 100, 172–182. https://doi.org/10.1016/j.gloplacha.2012.10.014.

Hatfield, J., Takle, G., Grotjahn, R., Holden, P., Liverman, D., Izaurralde, R.C, Mader, T. and Marshall, E. (2014) Agriculture. Melillo, J.M, Richmond, T.C & Yohe, G.W., *Climate change impacts in the united states*. The third national climate assessment. U.S. Global Climate Research Program, 150–174. https://

10970088, 2022, 4, Downloaded from https://rmets.onlinelibrary.wiley.com/doi/10.1002/joc.7378 by Johns Hopkins University, Wiley Online Library on [28/12/2022]. See the Terms and Conditions (https://onlinelibrary.wiley.com/terms-and-conditions) on Wiley Online Library for rules of use; OA articles are governed by the applicable Creative Commons License

nca2014.globalchange.gov/downloads/high/NCA3_Climate_Change_Impacts_in_the_United%20States_HighRes.pdf

Hatfield, J.L., Boote, K.J., Kimball, B.A., Ziska, L.H. and Wolfe, D. (2011) Climate impacts on agriculture: implications for crop production. *Agronomy Journal*, 103(2), 351–370.

Hatfield, J.L. and Prueger, J.H. (2015) Temperature extremes: effect on plant growth and development. *Weather and Climate Extremes*, 10, 4–10. https://doi.org/10.1016/j.wace.2015.08.001.

Karl, T.R., Nicholls, N. and Ghazi, A. (1999) Clivar/GCOS/WMO workshop on indices and indicators for climate extremes workshop summary. *Climate Change*, 42(1), 3–7.

Katz, R.W. and Brown, B.G. (1992) Extreme events in a changing climate: variability is more important than averages. *Climatic Change*, 21, 289–302.

Keggenhoff, I., Elizbarashvili, M., Amiri-Farahani, A. and King, L. (2014) Trends in daily temperature and precipitation extremes over Georgia, 1971-2010. *Weather and Climate Extremes*, Elsevier, 4, 75–85. https://doi.org/10.1016/j.wace.2014.05.001.

Kim, Y. and Lee, B. (2019) Differential mechanisms of potato yield loss induced by high day and night temperatures during tuber initiation and bulking: photosynthesis and tuber growth. *Frontiers in Plant Science*, 10(March), 1–9. https://doi.org/10.3389/fpls.2019.00300.

Kiros, G., Shetty, A. and Nandagiri, L. (2017) Extreme rainfall signatures under changing climate in semi-arid northern highlands of Ethiopia. *Cogent Geoscience*, 3(1), 1–20. https://doi.org/10.1080/23312041.2017.1353719.

Li, G., Yu, M., Fang, T., Cao, S. and Yan, L. (2013) Vernalization requirement duration in winter wheat is controlled by TaVRN-A1 at the protein level. *Plant Journal*, 76(5), 742–753. https://doi.org/10.1111/tpj.12326.

Liu, K., Baskin, J.M., Baskin, C.C., Bu, H. and Ma, M. (2013) Effect of diurnal fluctuating versus constant temperatures on germination of 445 species from the eastern Tibet plateau. *PLoS One*, 8(7), 1–10. https://doi.org/10.1371/journal.pone.0069364.

Mann, H.B. (1945). Nonparametric Tests Against Trend. Author(s): Henry B. Mann. Published by: The Econometric Society Stable. REFERENCES: Linked references are available on JSTOR for this article: You may need to log in to JSTOR, 13(3): 245–259. URL: https://www.jstor.org/stable/1907187.

Mann, M.L. and Warner, J.M. (2017) Ethiopian wheat yield and yield gap estimation: a spatially explicit small area integrated data approach. *Field Crops Research*. Elsevier B.V, 201, 60–74. https://doi.org/10.1016/j.fcr.2016.10.014.

Maraun, D. (2016) Bias correcting climate change simulations - a critical review. *Current Climate Change Reports*, 2, 211–220. https://doi.org/10.1007/s40641-016-0050-x.

Medvigy, D., Walko, R.L. and Avissar, R. (2012) Simulated links between deforestation and extreme cold events in South America. *Journal of Climate*, 25(11), 3851–3866. https://doi.org/10.1175/JCLI-D-11-00259.1.

Mekasha, A., Tesfaye, K. and Duncan, A.J. (2014) Trends in daily observed temperature and precipitation extremes over three Ethiopian eco-environments. *International Journal of Climatology*, 34(6), 1990–1999. https://doi.org/10.1002/joc.3816.

Mouhamed, L., Traore, S.B., Alhassane, A. and Sarr, B. (2013) Evolution of some observed climate extremes in the west African Sahel. *Weather and Climate Extremes*, 1, 19–25. https://doi.org/10.1016/j.wace.2013.07.005.

Navarro-racines, C., Tarapues, J., Thornton, P., Jarvis, A. and Ra, J. (2020) High-resolution and bias-corrected CMIP5 projections for climate change impact assessments. *Scientific Data*, 7, 1–14. https://doi.org/10.1038/s41597-019-0343-8.

Nyssen, J., Vandenreyken, H., Poesen, J., Moeyersons, J. and Govers, G. (2005) Rainfall erosivity and variability in the northern Ethiopian highlands. *Journal of Hydrology*, 311(1–4), 172–187. https://doi.org/10.1016/j.jhydrol.2004.12.016.

Omey, E., Mallor, F. and Nualart, E. (2009). An introduction to statistical modelling of extreme values. Application to calculate extreme wind speeds. Hub research paper, (November): 45. https://doi.org/10.1198/jasa.2002.s232.

Patterson, D.T., Westbrook, J.K., Joyce, R.J.V., Lingren, P.D. and Rogasik, J. (1999) Weeds, insects, and diseases. *Climatic Change*, 43, 711–727. https://doi.org/10.1023/A:1005549400875

Philip, S., Kew, S.F., van Oldenborgh, G.J., Otto, F. and Chris Funk H.C. (2017). The drought in Ethiopia, 2015: climate and development knowledge network and world weather attribution initiative: raising risk awareness. Royal Netherlands Meteorological Institute (KNMI), 1–7.

Philip, S., Kew, S.F., van Oldenborgh, G.J., Otto, F., O'Keefe, S., Haustein, K., King, A., Zegeye, A., Eshetu, Z., Hailemariam, K., Singh, R., Jjemba, E., and Funk, C. (2018) Attribution analysis of the ethiopian drought of 2015. *Journal of climate*, 31(6), 2465–2486. https://doi.org/10.1175/JCLI-D-17-0274.1

Piani, C., Haerter, J.O. and Coppola, E. (2010) Statistical bias correction for daily precipitation in regional climate models over Europe. *Theoretical and Applied Climatology*, 99, 187–192. https://doi.org/10.1007/s00704-009-0134-9.

Rosbakh, S. and Poschlod, P. (2015) Initial temperature of seed germination as related to species occurrence along a temperature gradient. *Functional Ecology*, 29, 5–14. https://doi.org/10.1111/1365-2435.12304.

Salmi, T., Maatta, A., Anttilaa, P., Ruoho-Airola, T. and Amnell, T. (2002). Detecting trends of annual values of atmospheric pollutatnts by the Mann-Kendall tests and Sen's slope estimates - the excel template application Makesens. Publications on air quality ATMOSPHERIC POLLUTANTS BY THE MANN-KENDALL. Finnish Meteorological Institute, 1–35.

Sen, P.K. (1968) Estimates of the regression coefficient based on Kendall's tau. *Journal of the American Statistical Association*, 63(324), 1379–1389.

Shang, H., Yan, J., Gebremichael, M. and Ayalew, S.M. (2011) Trend analysis of extreme precipitation in the northwestern highlands of Ethiopia with a case study of Debre Markos. *Hydrology and Earth System Sciences*, 15(6), 1937–1944. https://doi.org/10.5194/hess-15-1937-2011.

Siam, M.S. and Eltahir, E.A.B. (2017) Climate change enhances interannual variability of the Nile river flow. *Nature Climate Change*, 7(5), 350–354. https://doi.org/10.1038/nclimate3273.

Sillmann, J. and Roeckner, E. (2008) Indices for extreme events in projections of anthropogenic climate change. *Climatic Change*, 86(1–2), 83–104. https://doi.org/10.1007/s10584-007-9308-6.

Simane, B., Zaitchik, B.F. and Foltz, J.D. (2016) Agroecosystem specific climate vulnerability analysis: application of the livelihood vulnerability index to a tropical highland region. *Mitigation and Adaptation Strategies for Global Change*, 21(1), 39–65. https://doi.org/10.1007/s11027-014-9568-1.

10970088, 2022, 4, Downloaded from https://rmets.onlinelibrary.wiley.com/doi/10.1002/joc.7378 by Johns Hopkins University, Wiley Online Library on [28/12/2022]. See the Terms and Conditions (https://onlinelibrary.wiley.com/terms-and-conditions) on Wiley Online Library for rules of use; OA articles are governed by the applicable Creative Commons License

Simane, B., Zaitchik, B.F. and Mesfin, D. (2012) Building climate resilience in the Blue Nile/Abay highlands: a framework for action. *International Journal of Environmental Research and Public Health*, 9(2), 610–631. https://doi.org/10.3390/ijerph9020610.

Simane, B., Zaitchik, B.F. and Ozdogan, M. (2013) Agroecosystem analysis of the choke mountain watersheds, Ethiopia. *Sustainability (Switzerland)*, 5(2), 592–616. https://doi.org/10.3390/su5020592.

Teegavarapu, R.S.V. and Chandramouli, V. (2005) Improved weighting methods, deterministic and stochastic data-driven models for estimation of missing precipitation records. *Journal of Hydrology*, 312(1–4), 191–206. https://doi.org/10.1016/j.jhydrol.2005.02.015.

Teshome, A. and Zhang, J. (2019) Increase of extreme drought over Ethiopia under climate warming. *Advances in Meteorology*, 2019, 1–18. https://doi.org/10.1155/2019/5235429.

Thrasher, B., Maurer, E.P., Mckellar, C. and Duffy, P.B. (2012) Technical note: bias correcting climate model simulated daily temperature extremes with quantile mapping. *Hydrology and Earth Science Systems*, 16(9), 3309–3314. https://doi.org/10.5194/hess-16-3309-2012.

van Vuuren, D.P., Edmonds, J., Kainuma, M., Riahi, K. and Rose, S.K. (2011) The representative concentration pathways: an overview. *Climatic Change*, 109(1), 5–31. https://doi.org/10.1007/s10584-011-0148-z.

Vogel, E., Donat, M.G., Alexander, L.V., Meinshausen, M. and Frieler, K. (2019) The effects of climate extremes on global agricultural yields. *Environmental Research Letters*. IOP Publishing, 14(5), 1–12. https://doi.org/10.1088/1748-9326/ab154b.

Vreugdenhil, D., Bradshaw, J., Gebhardt, C., Govers, F., Taylor, M., MacKerron, D., and Ross, H.A. (2007) *Potato Biology and Biotechnology: Advances and Perspectives*.Amsterdam, The Netherlands: Elsevier.

Wang, X.L. (2008a) Penalized maximal F test for detecting undocumented mean shift without trend change. *Journal of Atmospheric and Oceanic Technology*, 25(3), 368–384. https://doi.org/10.1175/2007JTECHA982.1.

Wang, X.L. (2008b) Accounting for autocorrelation in detecting mean shifts in climate data series using the penalized maximal t or F test. *Journal of Applied Meteorology and Climatology*, 47(9), 2423–2444. https://doi.org/10.1175/2008JAMC1741.1.

Wang, X.L., Chen, H., Wu, Y., Feng, Y. and Pu, Q. (2010) New techniques for the detection and adjustment of shifts in daily precipitation data series. *Journal of Applied Meteorology and Climatology*, 49(12), 2416–2436. https://doi.org/10.1175/2010JAMC2376.1.

Wang, X.L. and Feng, Y. (2013). User Manual By. *Transform*, (July): 1–29.

Willmott, C.J. (1982) Some comments on the evaluation of model performance. *Bulletin of the American Meteorologcal society*, 63(11), 1309–1317.

Wold Bank. (2019). Disaster Risk Profile of Ethiopia.

World Bank. (2011). Climate Risk and Adaptation Country Profile Climate Investment Funds Climate Risk and Adaptation Country Profile Ethiopia COUNTRY OVERVIEW.

Zaitchik, B.F., Simane, B., Habib, S., Anderson, M.C. and Foltz, J.D. (2012) Building climate resilience in the Blue Nile/Abay highlands: a role for earth system sciences. *International Journal of Environmental Research and Public Health*, 9(2), 435–461. https://doi.org/10.3390/ijerph9020435.

Zhao, C., Liu, B., Piao, S., Wang, X. and Asseng, S. (2017) Temperature increase reduces global yields of major crops in four independent estimates. *Proceedings of the National Academy of Sciences*, 114(35), 9326–9331. https://doi.org/10.1073/pnas.1701762114.

Ziska, L.H. and Runion, G.B. (2007) Future weed, pest and disease problems for plants. In: Newton, P.C.D., Carran, R.A., Edwards, G.R. and Niklaus, P.A. (Eds.) *Agroecosystems in a changing climate*. Boca Raton, FL: CRC Press, pp. 261–287.

SUPPORTING INFORMATION

Additional supporting information may be found in the online version of the article at the publisher's website.

How to cite this article: Birhan, D. A., Zaitchik, B. F., Fantaye, K. T., Birhanu, B. S., Damot, G. A., & Tsegaye, E. A. (2022). Observed and projected trends in climate extremes in a tropical highland region: An agroecosystem perspective. *International Journal of Climatology*, *42*(4), 2493–2513. https://doi.org/10.1002/joc.7378

10970088, 2022, 4, Downloaded from https://rmets.onlinelibrary.wiley.com/doi/10.1002/joc.7378 by Johns Hopkins University, Wiley Online Library on [28/12/2022]. See the Terms and Conditions (https://onlinelibrary.wiley.com/terms-and-conditions) on Wiley Online Library for rules of use; OA articles are governed by the applicable Creative Commons License